Ankle joint stiffness during phases of human walking

Maciej Plocharski, Piotr Plocharski, group 13gr1076

June 4, 2013

Abstract

Joint stiffness relates the dynamic relationship between joint position and the torque acting about it, and thus is one of the factors that characterises the mechanical properties of a joint. Understanding the biomechanics of human ankle joint in dynamic conditions allows insight into design of ankle prostheses which could theoretically provide a functionality similar to that of a healthy limb. 11 non-disabled subjects (24-27 years) participated in the study. Subjects walked on a treadmill while perturbations (single displacement pulses) were applied to the ankle and the resulting torque was measured. Ankle joint stiffness was investigated during walking conditions in three phases of gait cycle, and in standing conditions, where subjects' leg postures isometrically matched the different phases of the dynamic trials.Stiffness estimates were generated using a multi-segment algorithm, with position and torque used to characterise the dynamic system non–parametrically. Results showed a non–significant difference between the mean values of joint stiffness during dynamic and isometric trials, and a statistically significant difference in mean ankle stiffness was found between the three phases of gait cycle at plantarflexion [$P < 0.0005$].

1 Introduction

IMPEDANCE of the human ankle joint has been consistently and successfully described with a second order system, consisting of an inertial, viscous and elastic component [Kearney et al., 1997, Mirbagheri et al., 2000, Ludvig et al., 2007]. Investigating joint impedance allows one to understand how a change in position of the joint translates into forces generated around that joint's axis of rotation.

The elastic component is referred to as joint stiffness, and it has been investigated with considerable interest in human ankle [Agarwal and Gottlieb, 1977, Kearney and Hunter, 1982, Hunter and Kearney, 1982, Fitzpatrick et al., 1992, de Zee and Voigt, 2001, Hansen et al., 2004]. It is component which dynamically translates the joint's angular position into the torque acting about it [Kearney et al., 1990] and thus it is a crucial characteristic in the control of movement and posture. Joint stiffness is determined by the intrinsic contributions of tissues and structures of the joint, muscles, tendons, ligaments, connective tissue, as well as the reflex contribution governed by the activation of muscles as part of the stretch and flexor reflex [Capaday, 2002].

Characterizing the modulation of joint stiffness and understanding how it varies during movement is very important in understanding how the nervous system regulates the mechanical properties of the limbs, the posture, and gait; it is vital in the control of movement, since the final position of a joint is controlled by the torque produced by the muscles [Ludvig and Kearney, 2007]. Therefore, investigating ankle joint stiffness in dynamic conditions may potentially aid the process of rehabilitating the function of the joint in response to loss of motor function. This contributes to designing ankle-foot prostheses that are intended to mimic the mechanical properties of the healthy limb in a manner that is biologically appropriate with the original ankle. Understanding ankle biomechanics and dynamics may lead to advances in design of prosthetic and orthotic devices, and improvements in the interaction between an amputee and a prosthesis [Hansen et al., 2004, Au et al., 2006].

The stiffness of a healthy human joint has received a lot of attention in research that utilises perturbations of torque or angular displacement and then examining the resulting angular displacements and torques [Agarwal and Gottlieb, 1977, Kearney and Hunter, 1982, Hunter and Kearney, 1982, Weiss et al., 1988]. The inertia, damping, and stiffness of the ankle can be approximated for various perturbations at

different ankle angles and for different levels of muscular activation around the ankle, using system identification techniques and assuming linearity [Kearney et al., 1990, 1997, Hansen et al., 2004, Ludvig and Perreault, 2011a]. Conventionally, such perturbation-based studies require a precise, rigid coupling between the limb and the perturbing/measuring equipment, while placing the limb inside a cast, which usually restrains natural gait and forces the subject to be rigidly attached to a servo-motor. This is very challenging to achieve in dynamic studies, which has led to walking and/or running studies based only on force platforms without applying perturbations, or treadmill perturbations [van Doornik and Sinkjær, 2007, Günther and Blickhan, 2002, Kuitunen et al., 2002].

The intrinsic stiffness of a joint has been shown to vary with the activation level of the associated muscles [Weiss et al., 1986, Sinkjaer et al., 1988, Kearney et al., 1990, Mirbagheri et al., 2000, Capaday, 2002]. It has been shown to change with position of the joint and the muscle activation level [Crowninshield et al., 1976, Zhang et al., 1997, Tai and Robinson, 1999, Mirbagheri et al., 2000], with the amplitude and velocity of the stretch [Stein and Kearney, 1995], and background torque [Sinkjaer et al., 1988, Mirbagheri et al., 2000].

A system developed by Andersen and Sinkjær [2003] provides an unique possibility of providing precise perturbations of the ankle joint, while evaluating the effect of a perturbation of the human ankle joint during a complete step cycle of walking [Sinkjær et al., 1996, Sinkjaer et al., 2004]. The main advantage of the device is that it allows a delivery of well-defined perturbations to ankle or knee joints throughout the entire gait cycle, and it measures the mechanics of the ankle joint perturbation during gait, while at the same time maintaining rigid control of the joint without affecting the normal gait pattern as it follows the ankle trajectory.

The time-varying behavior of joint stiffness has been observed in the human elbow [Bennett et al., 1992], as well as in knee joint studies [Zhang et al., 1997, Tai and Robinson, 1999, Ludvig et al., 2012], which recognizes the need for time-varying approaches in the study of ankle stiffness. The aim of our study was therefore to investigate the ankle stiffness in dynamic conditions during walking, and characterise the ankle joint stiffness in response to perturbations during three phases of the gait cycle: two during the stance phase and one during the swing phase for both dorsiflexion, and plantarflexion. Then, the ankle joint stiffness response to perturbations in isometric conditions was investigated, where perturbations were applied to standing subjects.

2 Methods

11 young non-disabled subjects, 9 males and 2 females participated in the study with an age range of 24-27 years. All subjects gave informed consent to the study.

2.1 Experiment materials

The centerpiece of the experimental setup for this study was the mobile ankle–and–knee perturbator, developed by Andersen and Sinkjaer [1995], which consists of a functional joint (Fig. 1) connected to an actuator by Bowden cables.

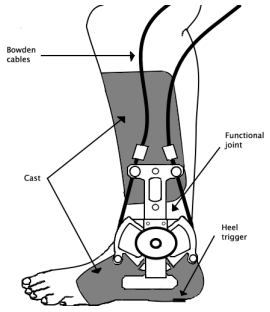

Figure 1: The functional joint mounted on the ankle.

A carbon–fiber epoxy casing was used as an interface between the functional joint and subjects' ankle. The casing was strapped around the calf and the underside of the left foot, lined with a durable stockinette to protect subjects from abrasion, and fastened with duct tape. The functional joint was aligned with the ankle joint's approximate axis of rotation.

The ankle–and–knee perturbator was placed next to a treadmill (Woodway USA, Inc.), (Fig. 2).

To measure the timing of the strides, as well as control the onset time of the perturbations, a force sensitive resistor was used as a heel trigger, taped underneath the left heel of the subject.

2.2 Experiment protocol

The ankle joint stiffness was investigated during both walking (dynamic) and standing (isometric) condi-

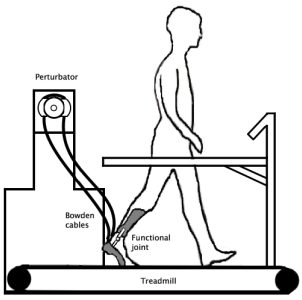

Figure 2: The experimental setup.

tions, to examine the stiffness modulation between these conditions. During the dynamic part, subjects were required to walk on the treadmill while the ankle joint was perturbed in three phases of gait cycle: at 20%, 50%, and 90% of the gait cycle. The isometric part of the experiment focused on position matching, where the subjects were standing on the treadmill in a posture that corresponded to precise positioning of the legs during these three phases. The perturbations were both dorsiflexions and plantarflexions, with amplitude and velocity specified in Table 1.

Parameter	Value
Amplitude	8°
Velocity	$300°/s$
Hold time	$200ms$

Table 1: Perturbation parameters used in the experiment.

Before either of the conditions was measured, a walking profile measurement was done, where 20 sweeps were recorded for each subject, while walking at a comfortable speed. The passive mode of the functional joint allowed following the ankle movement without interfering or changing the natural gait pattern. The average stride duration was extracted from the heel switch data to calculate precisely when in the gait cycle the perturbations were to be applied. Simultaneously, a video recording of a single stride was made with a camera placed next to the treadmill. The recording was analysed to extract the precise position of both feet on the treadmill at 20%, 50%, and 90% of the stride, which were then used during the isometric part of the experiment.

The order of which type of the experiment was carried out first, and the order of gait phase perturbation and was randomised.

2.2.1 Dynamic experiment

Subjects were required to walk on the treadmill with a preferred walking speed (3.840 ± 0.146 km/h). Perturbations (Table 1) were applied every 5-10 strides with a single displacement pulse during the gait cycle. To help the subjects maintain the rhythm of walking with a constant speed, a metronome was used. The length of the stride for each subject was monitored during the experiment to ensure that the stride duration did not change considerably during the length of the experiment, thus possibly resulting in an incorrect perturbation-application timing.

Measurements were collected until 20 correct sweeps of each gait phase perturbation, as well as perturbation direction, were recorded. Additionally, 20 sweeps without perturbation were recorded for each experiment combination to provide control data for comparison, and to monitor the subjects' gait duration.

2.2.2 Isometric experiment

Additionaly, subjects were instructed to stand still in positions mimicking the respective three phases of gait also examined in the dynamic experiment, i.e. at 20%, 50% and 90% of gait. The gait video recordings were used to determine the exact leg position and distance between the subjects' feet on the treadmill. The subjects were allowed to hold on to a railing during standing to provide stability, as it was assumed, that the effect of it on the ankle joint dynamics would be minimal. Perturbations were then applied to the ankle joint while stationary.

20 sweeps of each experiment combination were collected. No additional control data were recorded during the isometric part of the experiment.

2.3 Data collection

All data were collected by Mr. Kick software, a scientific data acquisition program, developed at Center for Sensory-Motor Interaction (SMI), Aalborg University, Denmark. The collected data were: electromyograph (EMG), joint angular position, torque acting around the joint, and heel trigger data. EMG data were collected using bipolar electrodes placed on the soleus (SOL) and the tibialis anterior (TA) muscles of the left leg. Data were sampled at 4 kHz by an analog–digital converter (ADC) in sweeps of 2 seconds each

and fed to a PC equipped with a data collection module (Data Acquisition Card PCL718). The EMGs were pre–amplified, digitally rectified and filtered from 0 to 40 Hz with a first-order Butterworth filter.

2.4 Data processing

The recorded position and torque data were used as input and output respectively to characterise the dynamic system non–parametrically, with its impulse response function (IRF). The system's output was represented by a two–sided discrete convolution, as follows:

$$y(i) = \Delta t \sum_{j=M_1}^{M_2} h(i,j)u(i-j) \tag{1}$$

where $y(i)$ was the output at sample i, $u(i)$ was the input at sample i, $h(i)$ was the IRF, j was the IRF lag, and M_1 and M_2 were the maximum and minimum lags. Since it is a time and computation intensive process to estimate the IRFs from data directly, as an alternative, the IRF was found between the position auto–correlation and the torque–position cross–correlation [Ludvig and Perreault, 2011b]. This gave the following:

$$\phi_{xy}(t,k) = \Delta t \sum_{j=M_1}^{M_2} \phi_{xx}(t-j,k-j)h(t,j) \tag{2}$$

where ϕ_{xy} is the torque–position cross–correlation, ϕ_{xx} is the position auto–correlation, and $h(t,j)$ is the time–varying IRF.

Solving Equation 2 for $h(t,j)$ yields the following:

$$h(t,j) = \Delta t^{-1} {\Phi_{xx}}^{-1} \phi_{xy} \tag{3}$$

where Φ_{xx} is symmetric Toeplitz matrix, and has the following form:

$$\Phi_{xx} = \begin{bmatrix} \phi_{xx}(t-M1,0) & \cdots & \\ \vdots & \ddots & \\ \phi_{xx}(t-M1,M2-M1) & \cdots & \\ \cdots & \phi_{xx}(t-M2,M1-M2) & \\ \ddots & \vdots & \\ \cdots & \phi_{xx}(t-M2,0) & \end{bmatrix} \tag{4}$$

and ϕ_{xy} is vector containing the position–torque cross–correlation:

$$\phi_{xy} = \begin{bmatrix} \phi_{xy}(t,M1) & \cdots & \phi_{xy}(t,M) \end{bmatrix} \tag{5}$$

Each position and torque data segment was aligned using the perturbation onset, and a window of 300 ms was extracted from the recorded data. Equation 3 was then used to calculate two–sided IRFs (4 lags on each side) from the position and torque windowed data. The area under the graph of the absolute value of the calculated IRFs for each sample point was calculated to get an estimate of the dynamic joint stiffness [Ludvig and Perreault, 2011a].

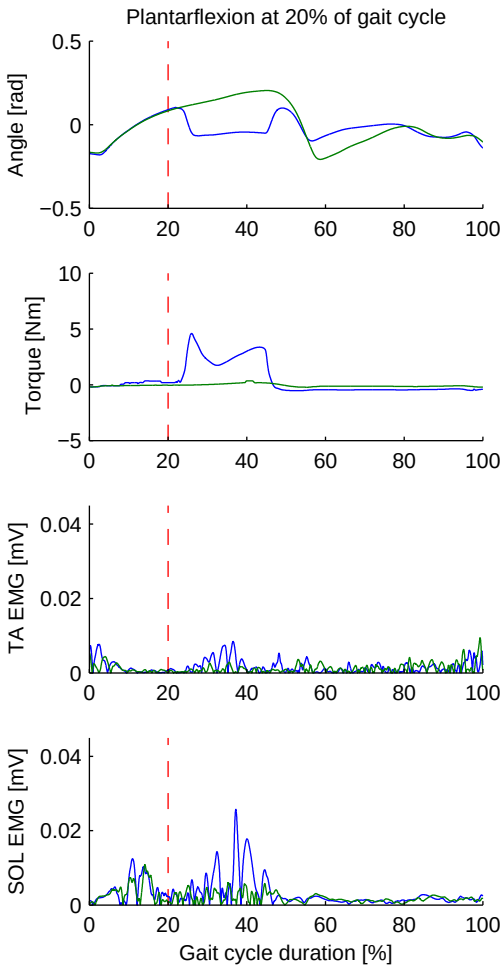

Figure 3: Example of data collected from a single subject. Blue line shows data from plantarflexion perturbation at 20% of gait cycle, green line shows data in absence of perturbation. Perturbation onset is marked by the vertical, dashed red line.

2.5 Statistical analysis

The collected data were analysed by means of a two–factor analysis of variance (ANOVA) and a subsequent Tukey HSD *post-hoc* analysis. The two examined factors were factor A: type of experiment (dynamic or isometric), and factor B: gait cycle phases (20%, 50%, and 90% of gait cycle duration).

3 Results

The data from the experiment were collected and analysed with the intention of investigating the modulation of ankle joint stiffness between standing (isometric) and walking (dynamic) conditions, as well as on the phase of the gait cycle in which a perturbation is applied to the joint. Additionally the effect of the alternating direction of the imposed perturbation (plantarflexion and dorsiflexion) was analysed.

The mean walking speed during the dynamic experiment was 3.84 km/s (SD=0.146 km/h, where SD is standard deviation). Subjects' mean gait cycle duration was 1.15 seconds (SD=0.07 seconds). Fig. 3 shows an example of data from a typical subject, averaged across repetitions (n=20) of plantarflexion perturbation at 20% of gait cycle. A change caused by a perturbation can be observed in the angle of the joint, the corresponding torque acting about the joint, and the EMG activities of the TA and SOL muscles when a perturbation was applied at the 20% of the gait cycle duration, which corresponded to 0.230 s of the gait cycle in that subject (20% of a 1.15s gait cycle, Subject 1).

The plantarflexion perturbation applied at time 20% resulted in torque increase, with a peak amplitude of 4.5 Nm. During the initial part of the perturbation, torque was dominated by the ineria and the intrinsic properties of the muscle–tendon complex around the joint [Sinkjaer et al., 1988]. The following additional increase in torque at about 115 ms after perturbation initiation onset (10% of gait duration after perturbation) was believed to be a SOL stretch reflex result [Sinkjær et al., 1996].

Fig. 4 shows examples of typical results from the experiment, from plantarflexion perturbation at 20% of gait cycle.

The maximum mean values of stiffness (K) in both dynamic and isometric trials were non-signifficantly different (two-factor ANOVA, [P = 0.77383]). K was observed to show disparity between dynamic and isometric trials during the initalization of perturbation (~t = 40 ms), and hold-release time (~ t = 270s). Between these two moments, the angular position was maintained constant during the hold time of 200 ms, and no change in angle resulted in dismissable K values.

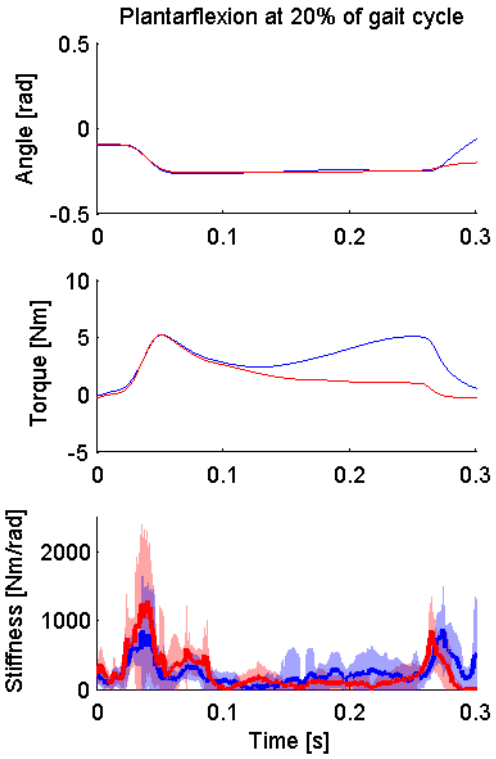

Figure 4: Summary of results from perturbations at 20% of gait cycle in plantarfelxion direction. Blue lines show results from dynamic trials; red lines show isometric results. Top and middle graphs are angular position and torque data, averaged across repeated sweeps (n=20) of individual subjects, and across all subjects (n=11). Bottom graph shows ankle joint stiffness averages from all subjects (n=11), with shaded areas showing ± 1 SD.

The observed values of stiffness were shown to vary between the dynamic and isometric trials at 20% of the gait cycle duration. The highest value of K was found during an isometric trial with a plantarflexion perturbation ($K = 1282 \pm 1028$ Nm/rad, at 41 ms after the perturbation onset). The reading was however taken at a point where the SD of the model estimations were large (see red shaded area on Fig. 4, bottom). At the exact same timing during the dynamic trial, maximum mean K was 707 ± 802 Nm/rad. During the hold-release time, both the isometric and dy-

Perturbation direction	$K_{Isometric} - K_{Dynamic}$	
	Initial phase	Hold release
20% Plantarflexion	575.2 [Nm/rad]	-17.7 [Nm/rad]
20% Dorsiflexion	12.6 [Nm/rad]	-142.3 [Nm/rad]
50% Plantarflexion	333.7 [Nm/rad]	330.3 [Nm/rad]
50% Dorsiflexion	-126.3 [Nm/rad]	478.4 [Nm/rad]
90% Plantarflexion	347.1 [Nm/rad]	-212.5 [Nm/rad]
90% Dorsiflexion	582.4 [Nm/rad]	-105.5 [Nm/rad]

Table 2: Summary of the ankle stiffness modulation investigated both during the dynamic experiment at three phases of gait cycle, and isometrically at the corresponding phase–matching postures. Values in the table signify the difference in mean stiffness values measured dynamically ($K_{Dynamic}$) and isometrically ($K_{Isometric}$).

namic stiffness values were within a close range of each other (859 ± 519 Nm/rad isometric at t = 266ms, and 877 ± 678 Nm/rad dynamic t = 274ms).

Differences between mean K values measured in dynamic and isometric conditions were observed during all phases of the gait cycle (Table 2. Positive numbers in Table 2 signify that mean K measured during the isometric experiment was higher than during the dynamic; if negative, K was lower. At perturbation-initalization (~t = 40 ms), maximum mean stiffness was lower in dynamic trials than in isometric for phases 20% and 90%, both plantar– and dorsiflexion, and in 50% for plantarflexion only.

At the end of each perturbation (hold-release time), measured mean K during isometric experiment was higher than during the dynamic in trials at 50% only (both plantar–, and dorsiflexion). Mean K was found to plateu during the hold period, with the exception the dorsiflexion perturbations at 50%.

Fig. 5 shows the comparison between stiffness values for perturbations between three phases of gait [$P < 0.0005$]. It can be seen that the highest stiffness values were estimated for the plantarflexion perturbations during 20% of gait cycle, both dynamic (877.0 ± 677.6 Nm/rad) and isometric (1283 ± 1029 Nm/rad), shown by blue lines on **A** and **C**, in Fig. 5.

Dorsiflexion results (**B** and **D**, in Fig. 5) showed more profound differences between the dynamic and isometric trials. The stiffness values for isometric trials exhibited distinct peaks at the initial phase, and after the hold phase, and a low plateau throughout the hold phase. However, the stiffness estimates for the dynamic dorsiflexion trials showed no common peak in the initial perturbation phase. The peak value for the dynamic dorsiflexion at 50% perturbation was found to be 705.0±925.9 Nm/rad, at t = 130 ms, which was during the perturbation hold phase.

4 Discussion

Experimental measurements of ankle stiffness during dynamic conditions such as unimpaired locomotion are of a great importance if one understanding how posture, gait and the mechanical properties of our limbs are regulated by the central nervous system.

Ankle joint stiffness has mostly been investigated during static conditions due to common experiment design limitations in walking studies, which involve a necessity to have the subject's limb attached rigidly while perturbed in a controlled manner. However, in order to properly understand the modulation of such stiffness during unimpaired gait, there is a need for dynamic experiments.

The use of the mobile ankle and knee perturbator in this study allowed successfully maintaining an unimpaired gait for the subjects while providing accurate perturbations to the ankle joint without impeding natural gait at the same time.

It was hypothesised that ankle joint stiffness measured during dynamic conditions would be lower than stiffness measured isometrically. The experimental design in this study allowed the estimation of stiffness during dynamic conditions of walking and then during isometric conditions, where the static posture matching provided the closest approximations of the corresponding conditions during walking.

Results showed a non–significant difference between the mean values of joint stiffness during dynamic and isometric trials. However, individually calculated mean stiffness values were found to have higher magnitudes for the isometric trials than those of the dynamic trials. This was most profound dur-

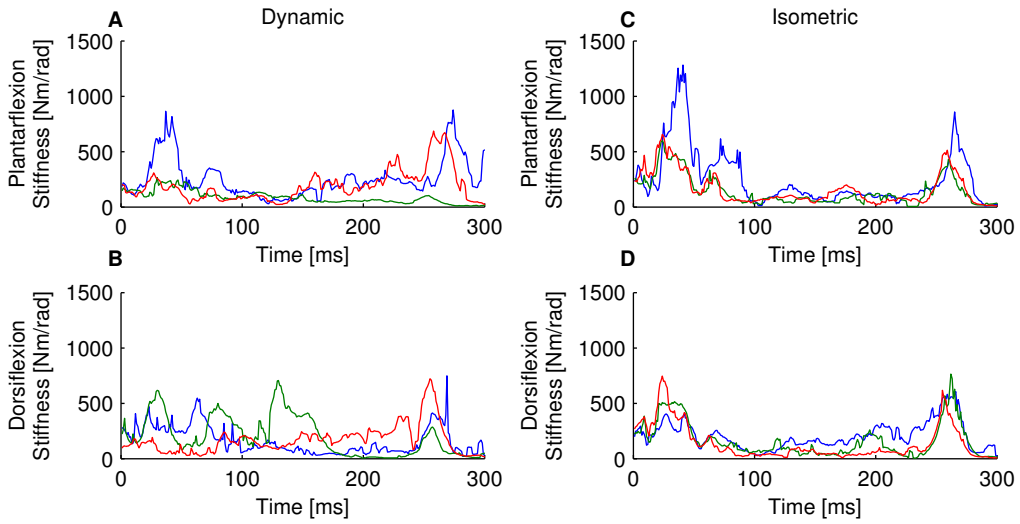

Figure 5: Summary of the ankle stiffness modulation investigated between phases of gait cycle during dynamic experiment (**A** and **B**), and isometric (**C** and **D**). Blue lines correspond to stiffness at 20% of gait cycle, green lines correspond to 50%, and red lines to 90%.

ing the initial perturbation phase (approximately between 0 ms and 80 ms) where the perturbation elicits the highest change in position and provokes a high torque variation.

Additionally, a statistically significant difference in mean ankle stiffness was found between the three phases of gait cycle during plantarflexion measurements only [two-factor ANOVA, $P < 0.0005$]. Tukey HSD *post-hoc* analysis showed that mean stiffness values were all different during the three phases of the gait cycle at plantarflexion. This is considered to be caused by the fact, that joint stiffness is modulated throughout the gait cycle. Since the three gait phases at which perturbations were applied are characterised by different conditions, such as joint angle, body weight support and contact with the ground, it was expected to find evidence of stiffness modulation between these conditions.

Literature suggests that joint stiffness is believed to be lower dynamic movement conditions when compared to static conditions, since neural control of movement is believed to be substantially different than that of posture Ludvig et al. [2012]. Indeed, Latash and Gottlieb [1991] and Bennett et al. [1992] reported that joint impedance was lower during movement than during fixed posture maintenance in human elbow joint. Ludvig et al. [2012] demonstrated that knee impedance during dynamic conditions was lower than would be predicted from isometric studies. Our results show a similar tendency for stiffness to be lower during dynamic experiments, where during perturbation-initalization, the maximum mean stiffness was lower in dynamic trials than in isometric for phases 20% and 90%, both plantar– and dorsiflexion, and in 50% for plantarflexion.

The study by Mirbagheri et al. [2000] analysed the intrinsic mean stiffness of the ankle joint in isometric conditions and found stiffness in range between the lowest value of 224 Nm/rad to the highest at 377 Nm/rad (with mean 325 Nm/rad and SD 72 Nm/rad) in trials involving pseudo-random binary sequence perturbations. When subjects were instructed to maintain a constant level of torque in a separate procedure, intrinsic stiffness reached the span between 310 Nm/rad and 509 Nm/rad (with mean 412 Nm/rad and SD 64 Nm/rad). Stiffness studies in dynamic conditions implementing force platforms reported K values of 5.68 Nm/deg in running 7.38 Nm/deg in sprinting respectively (325 Nm/rad and 422.8 respectively) [Stefanyshyn and Nigg, 1998]. Kuitunen et al. [2002] showed that ankle joint stiffness increased from 974 to 1375 Nm/rad with increasing running speed. Mean stiffness estimates in our study were therefore within the order of magnitude comparable to results found in literature.

References

GC Agarwal and CL Gottlieb. Compliance of the human ankle joint. *Journal of Biomechanical Engineering*, 99:166, 1977.

Jacob Buus Andersen and Thomas Sinkjaer. An actuator system for investigating electrophysiological and biomechanical features around the human ankle joint during gait. *Rehabilitation Engineering, IEEE Transactions on*, 3(4):299–306, 1995.

Jacob Buus Andersen and Thomas Sinkjær. Mobile ankle and knee perturbator. *Biomedical Engineering, IEEE Transactions on*, 50 (10):1208–1211, 2003.

Samuel K Au, Peter Dilworth, and Hugh Herr. An ankle-foot emulation system for the study of human walking biomechanics. In *Robotics and Automation, 2006. ICRA 2006. Proceedings 2006 IEEE International Conference on*, pages 2939–2945. IEEE, 2006.

DJ Bennett, JM Hollerbach, Y. Xu, and IW Hunter. Time-varying stiffness of human elbow joint during cyclic voluntary movement. *Experimental Brain Research*, 88(2):433–442, 1992.

Charles Capaday. The special nature of human walking and its neural control. *Trends in neurosciences*, 25(7):370–376, 2002.

R. Crowninshield, MH Pope, and RJ Johnson. An analytical model of the knee. *Journal of Biomechanics*, 9(6):397–405, 1976.

Mark de Zee and Michael Voigt. Moment dependency of the series elastic stiffness in the human plantar flexors measured in vivo. *Journal of biomechanics*, 34(11):1399–1406, 2001.

RC Fitzpatrick, JL Taylor, and DI McCloskey. Ankle stiffness of standing humans in response to imperceptible perturbation: reflex and task-dependent components. *The Journal of physiology*, 454(1):533–547, 1992.

Michael Günther and Reinhard Blickhan. Joint stiffness of the ankle and the knee in running. *Journal of biomechanics*, 35(11):1459–1474, 2002.

Andrew H Hansen, Dudley S Childress, Steve C Miff, Steven A Gard, and Kent P Mesplay. The human ankle during walking: implications for design of biomimetic ankle prostheses. *Journal of biomechanics*, 37(10):1467–1474, 2004.

IW Hunter and RE Kearney. Dynamics of human ankle stiffness: variation with mean ankle torque. *Journal of Biomechanics*, 15 (10):747–752, 1982.

RE Kearney and IW Hunter. Dynamics of human ankle stiffness: variation with displacement amplitude. *Journal of biomechanics*, 15(10):753–756, 1982.

Robert E Kearney, Ian W Hunter, et al. System identification of human joint dynamics. *Critical reviews in biomedical engineering*, 18(1):55, 1990.

Robert E Kearney, Richard B Stein, and Luckshman Parameswaran. Identification of intrinsic and reflex contributions to human ankle stiffness dynamics. *Biomedical Engineering, IEEE Transactions on*, 44(6):493–504, 1997.

Sami Kuitunen, Paavo V Komi, Heikki Kyrolainen, et al. Knee and ankle joint stiffness in sprint running. *Medicine and science in sports and exercise*, 34(1):166–173, 2002.

ML Latash and GL Gottlieb. Reconstruction of shifting elbow joint compliant characteristics during fast and slow movements. *Neuroscience*, 43(2):697–712, 1991.

D. Ludvig and R.E. Kearney. Real-time estimation of intrinsic and reflex stiffness. *Biomedical Engineering, IEEE Transactions on*, 54(10):1875–1884, 2007.

D. Ludvig and E. Perreault. System identification of physiological systems using short data segments. 2011a.

D. Ludvig and E.J. Perreault. Estimation of joint impedance using short data segments. In *Engineering in Medicine and Biology Society, EMBC, 2011 Annual International Conference of the IEEE*, pages 4120–4123. IEEE, 2011b.

D. Ludvig, S. Pfeifer, X. Hu, and E.J. Perreault. Time-varying system identification for understanding the control of human knee impedance. In *System Identification*, volume 16, pages 1306–1310, 2012.

Daniel Ludvig, Ian Cathers, and Robert E Kearney. Voluntary modulation of human stretch reflexes. *Experimental Brain Research*, 183(2):201–213, 2007.

MM Mirbagheri, H. Barbeau, and RE Kearney. Intrinsic and reflex contributions to human ankle stiffness: variation with activation level and position. *Experimental brain research*, 135(4):423–436, 2000.

T. Sinkjaer, E. Toft, S. Andreassen, and B.C. Hornemann. Muscle stiffness in human ankle dorsiflexors: intrinsic and reflex components. *Journal of Neurophysiology*, 60(3):1110–1121, 1988.

Thomas Sinkjær, Jacob Buus Andersen, and Birgit Larsen. Soleus stretch reflex modulation during gait in humans. *Journal of Neurophysiology*, 76(2):1112–1120, 1996.

Thomas Sinkjaer, Jacob Buus Andersen, Michel Ladouceur, Lars OD Christensen, and Jens Bo Nielsen. Major role for sensory feedback in soleus emg activity in the stance phase of walking in man. *The Journal of physiology*, 523(3):817–827, 2004.

Darren J Stefanyshyn and BM Nigg. Dynamic angular stiffness of the ankle joint during running and sprinting. *Journal of applied biomechanics*, 14:292–299, 1998.

RB Stein and RE Kearney. Nonlinear behavior of muscle reflexes at the human ankle joint. *Journal of neurophysiology*, 73(1):65–72, 1995.

C. Tai and C.J. Robinson. Knee elasticity influenced by joint angle and perturbation intensity. *Rehabilitation Engineering, IEEE Transactions on*, 7(1):111–115, 1999.

Johan van Doornik and Thomas Sinkjær. Robotic platform for human gait analysis. *Biomedical Engineering, IEEE Transactions on*, 54(9):1696–1702, 2007.

PL Weiss, RE Kearney, and IW Hunter. Position dependence of stretch reflex dynamics at the human ankle. *Experimental brain research*, 63(1):49–59, 1986.

PL Weiss, IW Hunter, and RE Kearney. Human ankle joint stiffness over the full range of muscle activation levels. *Journal of biomechanics*, 21(7):539–544, 1988.

L.Q. Zhang, G. Nuber, J. Butler, M. Bowen, and W.Z. Rymer. In vivo human knee joint dynamic properties as functions of muscle contraction and joint position. *Journal of biomechanics*, 31(1): 71–76, 1997.

AALBORG UNIVERSITY
DENMARK

ANKLE JOINT STIFFNESS DURING PHASES OF HUMAN WALKING

Master thesis

Group 13gr1076

Maciej Plocharski Piotr Plocharski

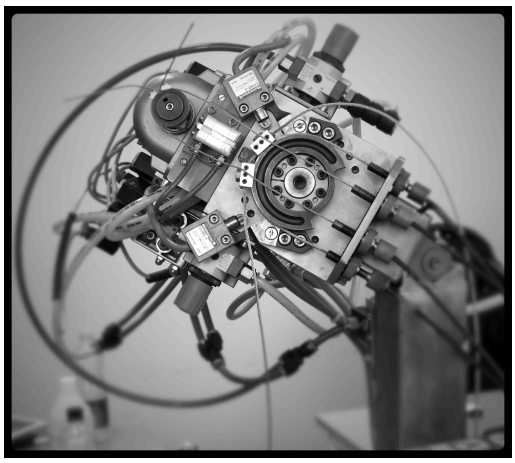

Biomedical Engineering and Informatics

AALBORG UNIVERSITY

Department of Health Science & Technology
Frederik Bajers Vej 7D2
9220 Aalborg SØ
Telephone (+45) 9940 9940
Fax (+45) 9815 4008
http://www.hst.aau.dk

Title:
Ankle joint stiffness during phases of human walking.

Theme:
Master thesis.

Project period:
4th semester Master, 2013
February 1st, 2013 - June 4th, 2013

Project group:
Group 13gr1076

Authors:
Maciej Plocharski
Piotr Plocharski

Project supervisors:
Mark de Zee
Ole Kæseler Andersen

No. printed Copies: 5

No. of Pages: 71

No. of Appendix Pages: 9

Total no. of pages: 80

Synopsis:

Understanding the biomechanics of human ankle joint in dynamic conditions allows insight into design of ankle prostheses which could theoretically provide a functionality similar to that of a healthy limb. Joint stiffness is one of the factors that characterises the mechanical properties of a joint, as it relates the dynamic relationship between joint position and the torque acting about it.
11 young non-disabled subjects (24-27 years) participated in the study. Subjects walked on a treadmill while perturbations (single displacement pulses) were applied to the ankle and the resulting torque was measured. Ankle joint stiffness was investigated during walking conditions in three phases of gait cycle, and in standing conditions, where subjects' leg postures isometrically matched the different phases of the dynamic trials. Stiffness estimates were generated using a multi-segment algorithm, with position and torque used to characterise the dynamic system non–parametrically.
Results showed a non–significant difference between the mean values of joint stiffness during dynamic and isometric trials, and a statistically significant difference in mean ankle stiffness was found between the three phases of gait cycle at plantarflexion [$P < 0.0005$].

Institut for Sundhedsvidenskab og Teknologi
Frederik Bajers Vej 7D2
9220 Aalborg SØ
Tlf. (+45) 9940 9940
Fax (+45) 9815 4008
http://www.hst.aau.dk

Titel:
Ankel ledstivhed i faser af gangcyklussen.

Tema:
Speciale projekt (4. Semester)

Projektperiode:
4th semester Master, 2013
February 1st, 2013 - June 4th, 2013

Projektgruppe:
Gruppe 13gr1076

Gruppemedlemmer:
Maciej Plocharski
Piotr Plocharski

Vejledere:
Mark de Zee
Ole Kæseler Andersen

Oplagstal: 5

Antal sider: 71

Antal sider i bilag: 9

Samlet antal sider i raporten: 80

Synopsis:

Forståelse og fortolkning af biomekanikken i menneskets ankelled under dynamiske forhold giver et indsigt i hvordan kunne designet af ankelproteser udvikles til det punkt, hvor funktionaliteten af det sunde ankel genskabes helt. Stivhed er én af de faktorer, der karakteriserer de mekaniske egenskaber af et led, da det formidler den dynamiske forhold mellem leddetsposition og momentet omkring leddet.
11 unge, sunde forsøgspersoner (24–27 år) deltog i studiet. Forsøgspersonerne gik på et løbebånd, mens perturbationer (enkle forskydnings pulser) var påført ankleleddet og det resulterende moment var målt. Ankelstivhed blev forsket under gående forhold i tre faser af gangcyklussen, og under stående forhold, hvor forsøgspersonernes ben positur matchede de tre faser under dynamiske forsøg. Stivhedsestimater blev genereret ved hjælp af en multi–segment algoritme, hvor position– og momentdata blev brugt til at karakterisere det dynamiske system non–parametrisk.
Resultater viste et statistisk ikke signifikant forskel mellem middleværdier for stivhed under dynamiske og statiske forsøg, samt en statistisk signifikant forskel mellem stivhed middleværdierne under plantarflexion perturbationer i de tre faser af gangcyklus [$P < 0.0005$].

ABSTRAKT

Det primære funktion i proteser til underbenet, hos patienter efter fod og ankel amputation, er så vidt muligt at genskabe funktionen og udseende af et mistede fod og ankel. Med udviklingen af aktive proteser har man nu mulighed for at designe og levere proteser til underbenet, der i høj grad genskaber funktionen af det sunde ben. En stor fordel af aktive proteser, er at de kan aktivt medvirke under gang og kan tilpasses til den enkle individ, så de frembringer den mest effektive og hurtige rehabilitation af underbenets funktion [Kapp et al. 2009]. Det er dog svært at indstille de mekaniske egenskaber af ankelproteser, på en måde der korrekt afspejler de biomekaniske egenskaber af ankelledsystemet.

Én af biologiske parametre, der bruges til at forstå den dynamiske virkning af ankelleddet er stivhed [Hunter & Kearney 1982]. Stivhed er én af komponenterne i forholdet, der kaldes impedans, som beskriver den dynamiske forhold mellem ændringen af leddets position og den resulterende moment omkring leddet. Stivhed har været i fokus for forskere i lang tid, med hensigt på at forstå biomekanikken i ankelleddet, samt andre led, som knæ og elbue [Kearney & Hunter 1982, Bennett et al. 1992, Ludvig et al. 2012].

Metoden til at evaluere stivhed under eksperimentalle forhold er baseret på perturbationer, der er meget hurtige impulser, der ændrer leddets position og forårsager en respons i momentet omkring leddet. Denne metode er dog meget udfordrende at implementere i forsøg, og er derfor hovedsageligt blevet beskrevet under statiske forsøg. En mobil ankel–og–knæ perturbator, udviklet af Andersen & Sinkjær [2003], giver nu muligheden for at udføre dynamiske forsøg, hvor præcise perturbationer kan påføres ankelleddet i forskellige faser af gangcyklussen.

Et forsøgsdesign blev udviklet, hvor ankelstivhed blev undersøgt i dynamiske forhold under gang, i løbet af tre forskellige faser af gangcyklussen, og blev bagefter sammenlignet med statiske forsøg under tilsvarende tre faser. 11 unge, sunde forsøgspersoner (24–27 år) deltog i studiet. Forsøgspersonerne gik på et løbebånd, mens perturbationer var påført ankleleddet og det resulterende moment var målt. Derudover blev målingerne taget mens forsøgspersonerne stod i tre ben positur, som matchede de tre faser fra dynamiske forsøg og perturbation blev pålagt ankelleddet. Stivhedsestimater blev genereret ved hjælp af en non–parametrisk metode, kaldt multi–segment algoritme. Position– og momentdata blev brugt til at karakterisere det dynamiske system ved hjælp af impuls respons funktioner.

Resultater viste et statistisk ikke signifikant forskel mellem middleværdier for stivhed under dynamiske og statiske forsøg, samt en statistisk signifikant forskel mellem stivhed middleværdierne under plantarflexion perturbationer i de tre faser af gangcyklus [$P < 0.0005$]. Resultaterne blev dog undersøgt mellem middleværdier for stivhed under dynamiske og statiske forhold. Der blev observeret en forskel på stivhed middleværdier mellem de to typer af forsøg. Stivhed un-

der de dynamiske forhold havde en lavere middleværdier end stivhed under de statiske i begyndelsen af perturbationsfasen.

Der var også observeret en forskel på stivhedsmiddleværdier mellem de tre faser af gangcyklussen, men kun i retning af plantarfleksion. På baggrund af resultaterne kan der konkluderes, at der et krav til at videreundersøge ankelledstivhed i de dynamiske forhold.

PREFACE

This report was written as worksheets documentation for a scientific article written as a 4th Master thesis M.Sc. by group 13gr1076, during the period of February 1st 2013 to June 4th 2013 at Aalborg University, in the field of Biomedical Engineering and Informatics, under the supervision of Mark de Zee and Ole Kaeseler Andersen. The worksheets provide additional information into the topic of human ankle stiffness, and present a thorough documentation of the work proces during the design, implementation of the experiment, and data analysis. The structure of the worksheets is arranged in a way which follows the structure of a project report.

The project concerns an investigation of the time-varying stiffness of the human ankle joint during dynamic conditions in order to gain an understanding of the ankle biomechanics which may lead to future advances in design of prosthetic and orthotic devices.

All citations in this report refer to the bibliography list at the end of the report. References are organized according to the Harvard method, [Author's last name, year of publishing].

This report was written by:

Maciej Plocharski

Piotr Plocharski

CONTENTS

Part I

Analysis

CHAPTER 1

INTRODUCTION

1.1 Anatomy of the ankle

The ankle, *tarsus*, is the region of the human body, where the foot is connected to the lower limb. The ankle joint is the site, where the bones of the lower leg, tibula and fibia, interact with the bones of the foot, primarily the talus, to transmit the weight of the body toward the toes [Martini & Nath 2009]. However, what is commonly known as the ankle, is not a single joint, and is instead called the *ankle joint complex* [Behnke 2006].

The movements carried out by the ankle joint complex can be divided into two categories: movements of the sagittal plane, i.e. plantarflexion and dorsiflexion, and movements of the frontal plane, i.e. inversion and aversion (see Figure 1.1). Motion in the sagittal plane is articulated by the talocrural aspect of the ankle joint complex, which is therefore considered the "true" ankle joint [Behnke 2006]. The frontal plane movements are articulated by the talocalcaneal, or subtalar, aspect of the ankle joint complex. For clarity, throughout this work, the expression "ankle joint" will refer to the talocrural aspect of the ankle joint.

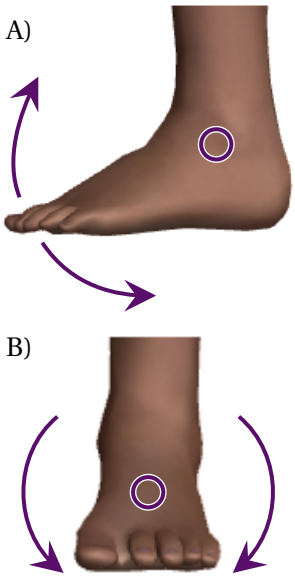

Figure 1.1: Motions of the ankle joint. A) Sagittal plane motion. B) Frontal plane motion. Figure adapted from Zygote Media Group [2013].

The ankle joint is a monoaxial diarthrosis, or synovial joint, meaning a freely movable joint, which permits movement in one plane [Martini & Nath 2009]. It allows the foot to be extended from the anterior surface of the tibia (plantarflexion) or flexed towards the anterior tibial surface (dorsiflexion) during motion. Like all synovial joints, the ankle joint is encapsulated in a synovial membrane, filled with synovial fluid. The bone surfaces, that would otherwise come in contact, such

as talus and tibia, are covered with articular cartilages and separated by a thin film of synovial fluid to reduce friction and protect the bone surfaces from mechanical damage [Martini & Nath 2009].

The following subsections will describe the bones (subsection 1.1.1), ligaments (subsection 1.1.2) and muscles of the ankle joint (subsection 1.1.3).

1.1.1 Bones of the ankle

The ankle joint is made up of seven bones, called the tarsal bones, which can be seen on Figure 1.2 [Martini & Nath 2009].

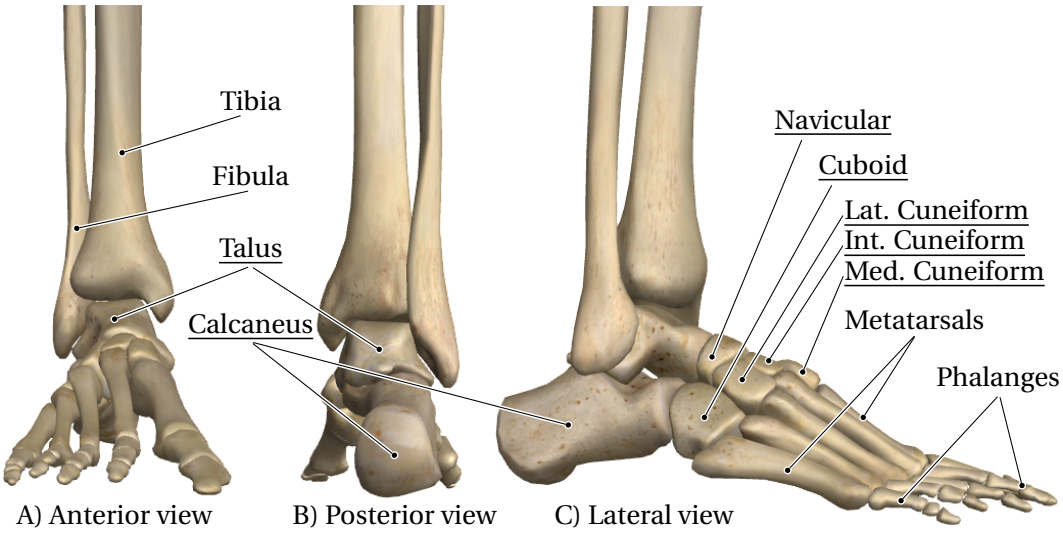

Figure 1.2: Bones of the ankle region. Tarsal bones are underlined. A) Anterior view of the ankle. B) Posterior view of the ankle. C) Lateral view of the ankle. Figure adapted from Zygote Media Group [2013].

The talus is the second largest bone of the ankle, and plays the lead role in articulating the ankle's movement. The superior surface process of the talus, called *trochlea tali*, has the shape of a pulley, that spans around 160° [Bojsen-Møller 2009]. The trochlea serves as the joint head, with the trochlea's superior and medial surfaces articulating with the tibia, and the lateral surface with the fibula [Martini & Nath 2009].

The calcaneus, or the heel bone, is the largest tarsal bone, and, during standing, serves to transit most of the body's weight to the ground. Together with the talus, they form the talocalcaneal aspect of the ankle joint complex, which allows lateral (aversion) and medial (inversion) movement of the foot [Behnke 2006]. The site on the calcaneus, where it articulates with the talus is the facies articularis talaris posterior. Also, the calcaneus is the attachment site for the calcaneal tendon, or Achilles tendon [Martini & Nath 2009].

The remaining tarsal bones are the cuboid, navicular and the medial, intermediate and lateral cuneiform bones. Together, these tarsal bones form the midfoot and articulate with the talus, calcaneus, each other and the metatarsal bones [Martini & Nath 2009].

1.1.2 Ligaments of the ankle

Ligaments are bundles of connective tissues, made up mostly of collagen fibers, which bind bones together. Ligaments are a type of dense regular connective tissue, which means that the collagen fibers are packed tightly, parallel to each other and aligned with the forces applied to the tissue that they support [Martini & Nath 2009]. See Figure 1.3 for an overview of the ankle ligaments.

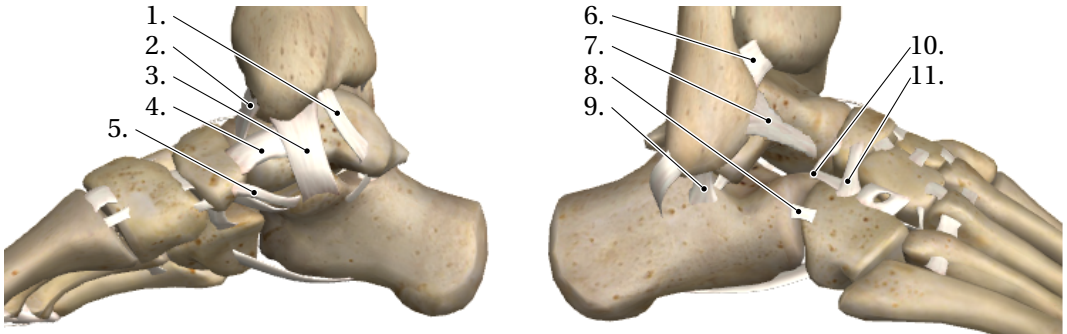

A) Medial view B) Lateral view

Figure 1.3: Ligaments of the ankle joint complex. A) Medial view of the ankle. 1. Posterior talotibial lig. 2. Anterior talotibial lig. 3. Calcaneotibial lig. 4. Tibionavicular lig. 5. Calcaneonavicular lig. B) Lateral view of the ankle. 6. Anterior tibiofibular lig. 7. Anterior talofibular lig. 8. Calcaneocuboid lig. 9. Calcaneofibular lig. 10. Bifurcated lig. 11. Cuboidenavicular lig. Figure adapted from Zygote Media Group [2013].

The ligaments of the ankle are named after the bones they connect, and are divided into groups called the *intertarsal ligaments*, and the *tarsometatarsal ligaments*. The intertarsal ligaments are responsible for holding the tarsal bones together and allow articulation of the ankle joint complex. On the medial side of the ankle, the ligaments form a complex called the *deltoid ligament* [Behnke 2006]. The ligaments forming the deltoid ligament are the tibionavicular ligament, the calcaneotibial, the posterior talotibial ligament and the anterior talotibial ligament (1.-4. on Figure 1.3).

On the lateral side of the ankle, there are ligament structures tying the tarsal bones to the fibula. Among these is the anterior talofibular ligament, binding the anterior side of the distal end of fibula to the talus, and is the most commonly sprained ligament in the ankle joint [Behnke 2006]. The strongest lateral ankle ligament is the posterior talofibular ligament (not visible on Figure 1.3), which binds the posterior side of fibula's distal end to the talus.

The tarsometatarsal ligaments bind the five metatarsal bones to the tarsal bones. The tarsometatarsal ligaments are made up of dorsal and plantar capsular, and interosseous ligaments, which form the joints between the metatarsals and the bones of the midfoot [Behnke 2006].

1.1.3 Muscles of the ankle

This subsection will examine the muscles acting around the ankle and controlling the four fundamental movements of the ankle joint complex– dorsiflexion, plantarflexion, eversion and inversion. The muscles that act about the ankle joint are extrinsic muscles, which means that they originate outside the foot, in the lower leg, and insert into the foot via tendons [Behnke

2006]. Muscles of the lower leg are grouped together according to their position, and bound by collagenous sheets of the superficial and deep fascia, in effect creating four isolated compartments [Martini & Nath 2009]. A list of the four compartments, as well as the muscles that are contained within can be found in Table 1.1.

Compartment	**Muscle**	**Action**
Anterior	Tibialis anterior	Dorsiflexion at ankle; inversion of the foot
	Extensor hallucis longus	Dorsiflexion at ankle; extension at joints of the great toe
	Extensor digitorum longus	Dorsiflexion at ankle; extension at joints of the remaining toes
	Fibularis tertius	Dorsiflexion at ankle; eversion of the foot
Lateral	Fibularis longus	Plantarflexion at ankle; eversion of the foot; support longitudinal arch
	Fibularis brevis	Plantarflexion at ankle; eversion of the foot
Superficial posterior	Gastrocnemius medialis & lateralis	Plantarflexion at ankle; inversion of foot; flexion at knee
	Soleus	Plantarflexion at ankle
	Plantaris	Plantarflexion at ankle; flexion at knee
Deep posterior	Popliteus	Rotation of tibia; flexion at knee
	Flexors hallucis longus	Flexion at joints of the great toe
	Flexir digitorum longus	Flexion at joints of the remaining toes
	Tibialis posterior	Plantarflexion at ankle; adduction and inversion of foot

Table 1.1: Muscles making up the four compartments in the lower leg, and their action. Muscle actions responsible for dorsi– and plantarflexion of ankle joint have been highlighted with colors: blue for dorsiflexion and green for plantarflexion.

A muscle's function can be determined by the placement of its tendon with regard to the axes of movement of the ankle joint complex. Muscles, whose tendons are attached anterior or posterior to the rotation axis of the talocrural joint are dorsi– or plantarflexors, respectively. Muscles with tendons on the lateral and medial side of the rotation axis of the talocalcaneal joint provoke an eversion or an inversion [Bojsen-Møller 2009].

Even though dorsi– and plantarflexion of the ankle joint are carried out by a collection of muscles (as seen on Table 1.1), there are muscles, which carry out the dominating part of the work in articulating the ankle joint. The main dorsiflexor is the tibialis anterior, while plantarflexion is mostly carried out by a group of muscles collectively called *triceps surae*, made up of the gastrocnemius medialis, the gastrocnemius lateralis and the soleus [Bojsen-Møller 2009].

The tibialis anterior originates at the proximal two-thirds of the shaft of tibia, on the lateral side. The head of the muscle follows the lateral side of the tibial shaft, and only in the distal end crosses in front of tibia and inserts on the medial side of the ankle. The distal tendon of tibialis anterior is attached at the medial cuneiform bone and the base of the first metatarsal bone [Martini & Nath 2009]. The tibialis anterior is capable of providing more work during dorsiflexion of the foot then the three other muscles of the anterior compartment together [Bojsen-Møller 2009].

The two heads of the gastrocnemius muscle originate just proximal to the knee, on the medial and lateral posterior femoral condyles. The lateral and medial heads combine over the distal half of the tibia and insert together through the Achilles tendon at the posterior of the calcaneus [Behnke 2006]. The soleus muscle originates at the proximal third of the posterior of the fibula and the posteromedial shaft of the tibia. It inserts together with the gastrocnemius muscle at Achilles tendon [Behnke 2006]. In the triceps surae muscle group, all the muscles generate high forces during plantarflexion the foot, but the soleus muscle, which is made up of short, slow muscle fibers, is mostly responsible for continuous maintaining and adjustments of posture [Martini & Nath 2009].

1.2 Gait cycle

The main purpose of locomotion, be in humans or animals, is moving the body's center of mass in a given, desired direction. Bipedal locomotion is a cyclic task, where each limb goes through two phases in each cycle. When any part of the foot is in contact with the ground, the phase is called stance, and when the foot is lifted, and there is no ground contact, the phase is called swing. Both phases are divided further down into specific elements, depending on which part of the foot is either achieving, or losing contact with the ground (in stance), or whether the foot accelerating, decelerating or where it is relative to the contralateral foot (in swing). A single stride, or a full completion of the gait cycle, is marked by a repeated occurrence of an event for a single limb. The stance phase is longer than swing phase, and usually occupies 60% of the stride duration [Nordin & Frankel 2012]. See Figure 1.4 for a diagram outlining the phases and events in the gait cycle.

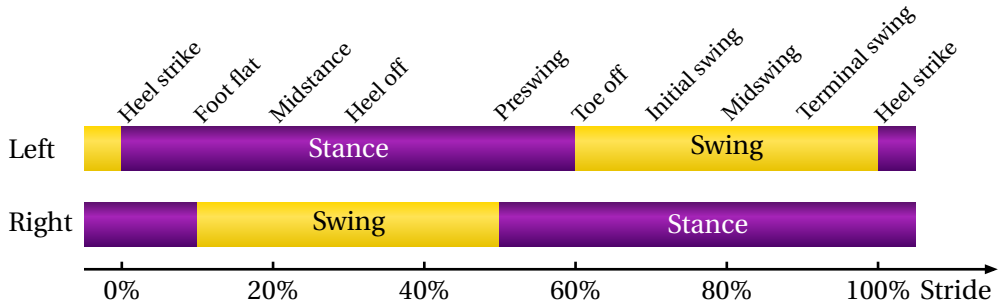

Figure 1.4: The phases and events of the gait cycle, for the left and right foot, shown over the stride duration.

There are six identifiable elements in the stance phase, consisting of events and periods. The first event, which is also commonly regarded as the beginning of a gait cycle is the *heel strike*, also called heel contact, where the foot first makes contact with the ground. After the heel touches ground, the leg prepares to take the weight of the body, and the foot comes down into full contact with the ground. This event is called *foot flat*, and occurs approximately at 10% of the stride. As the head, arms and trunk (HAT) continue moving forward, they pivot towards the weight bearing foot, while the contralateral limb begins its swing phase. As the center of gravity is above the weight bearing foot, the period is called *midstance*, and lasts from 10% to 30% of the stride. The next period is the *heel off*, where the foot prepares to push off the ground, the heel is lifted of the ground and the weight of the body is transferred on the mid– and forefoot regions. This period lasts from 30% till 50% of the stride. The last period of the

stance phase, lasting from 50% to 60% of the stride, is the *preswing*, where the weight of the body is transferred onto the contralateral foot. At approximately 60% of the stride comes the *toe off*, where the foot is lifted off the ground, and the swing phase begins [Donatelli 1996].

The swing phase lacks identifiable events, and is instead divided into three, approximately equal periods [Nordin & Frankel 2012]. The first period, called *initial swing*, is the acceleration phase, and lasts approximately from 60% to 73% of the stride. The next period, called *midswing*, coincides with the midstance period of the contralateral foot and last from 73% till 87%. It ends when the ipsilateral tibia passes the vertical position. The last period is called *terminal swing* and is the deceleration phase lasting from 87% to 100% of the stride [Donatelli 1996].

CHAPTER 2

ANKLE STIFFNESS

During unimpaired gait, able-bodied individuals vary the forces generated by their lower limbs, as well as the stiffness of that limb. Studies have shown that humans adjust leg stiffness to accommodate surface changes during hopping in place, and forward running [Ferris & Farley 1997, Ferris et al. 1998]. It has been also shown that there is evidence that modulation of ankle stiffness is the primary mechanism for adjusting leg stiffness under a variety of circumstances [Farley et al. 1998].

A person's locomotion depends for example on the terrain or the obstacles one may encounter during walking. Therefore, a person can either walk in a relaxed manner, or may suddenly stiffen up the joints, either in order to increase stability or as a method for shock or impact absorption [Roy et al. 2011].

The stability of the ankle joint has received a share of interest among researchers, as it plays an important role in maintaining stability of the ankle during unimpaired walking. This stability is influenced by passive mechanisms such as stiffness of ligaments, as well as active and neuromotor mechanisms, such as reflex and voluntary control. Joint stiffness can be categorized on the basis of whether it is measured under passive or active conditions. Passive stiffness is described as the resistance to shortening or elongation; in the context of biomechanics it refers to the mechanical stiffness that is provided by the combination of the joint, tendon, and the connective tissue. Active stiffness is a function of muscle activation contraction of the muscle fibers mediated through the stretch reflex [Capaday 2002, Roy et al. 2011].

Joint stiffness is a component of joint impedance, which is an important property of the human muscular system, and it plays a very important role in movement and posture control. Joint impedance relates the position of the joint and the torque acting about that joint. It has been consistently and successfully described with a second order system, consisting of an inertial, viscous and elastic component [Kearney et al. 1997, Mirbagheri et al. 2000, Ludvig et al. 2007]. Investigating joint impedance allows one to understand how a change in position of the joint translates into forces generated around that joint's axis of rotation.

It has been established that the mechanics of the joints vary under different conditions. While

joint impedance can be successfully characterized during isometric, time-invariant conditions, it is known to fluctuate while the limb is in movement, since the position of the joint and the activity of the surrounding muscles vary in time [Zhang et al. 1997, Mirbagheri et al. 2000]. The dynamic joint impedance is a property of a system that maps the relation between the angle or position of the joint and the torque acting about that joint; and it includes resistance to such dynamic factors as displacement, velocity, and acceleration [Ludvig & Perreault 2011a, Roy et al. 2011]. The intrinsic joint stiffness is a property that provides a torque response to any change in the angle of the joint under study without any intervention from the nervous system, as it is a rapid mechanical stiffness provided by the combination of active muscle, tendon, and connective tissue [Loram & Lakie 2002]. It is debated whether the intrinsic ankle stiffness is modulated by the nervous system [Gatev et al. 2004] or not, or rather is a biomechanical constant [Loram & Lakie 2002].

Characterizing the modulation of joint stiffness and understanding how it varies during movement is very important in understanding how the nervous system regulates the mechanical properties of the limbs, the posture, and gait [Ludvig & Kearney 2007]. For example, it has been shown that the non-disabled human ankle appears to change stiffness characteristics as gait speed changes [Hansen et al. 2004]. There is also substantial proof by Lark et al. [2003]that ankle joint stiffness plays a crucial role during the single support phase to control forward and downward body momentum.

The common approach to measuring stiffness of the able-bodied human has been by means of perturbations of torque or position displacements. This method has been used in the measurements of stiffness in other joints such as the elbow joint [Latash & Gottlieb 1991, Bennett et al. 1992, Abe & Yamada 2003, Ludvig & Perreault 2011b, Hu et al. 2011], and knee joint [Zhang et al. 1997, Tai & Robinson 1999, Ludvig et al. 2012, Pfeifer et al. 2012]. Stiffness of the ankle joint has also been investigated using perturbation approach and examining the torque and angular displacement [Agarwal & Gottlieb 1977, Kearney & Hunter 1982, Hunter & Kearney 1982, Weiss et al. 1988].

However, the complexities of the ankle stiffness modulation during walking have not yet been fully investigated. Lower limb stiffness proves to be hard to estimate during locomotion. Joint stiffness depends very strongly on both voluntary contraction of the muscles around the joint as well as the angular position of the joint and it has been shown to change at different velocities [Hansen et al. 2004]. For example, the intrinsic stiffness of a joint has been shown to vary with the activation level of the associated muscles [Weiss et al. 1986, Sinkjaer et al. 1988, Kearney et al. 1990, Mirbagheri et al. 2000, Capaday 2002]. What is more, it also changes with position of the joint and the muscle activation level change as well [Crowninshield et al. 1976, Zhang et al. 1997, Tai & Robinson 1999, Mirbagheri et al. 2000]. Changes in amplitude and velocity of the stretch also have an impact on joint stiffness [Stein & Kearney 1995]. Finally, changes in background torque result in joint stiffness variations [Sinkjaer et al. 1988, Mirbagheri et al. 2000].

2.1 Methods of estimation

System identification techniques can be used to approximate the dynamic properties of the ankle joint. The dynamic relationship between the joint torque and angular displacement is

quantified using limb inertia, viscosity and joint stiffness, and has been used in literature to approximate for perturbation studies at different angles of the ankle joint and for different levels of muscle activation around the ankle [Mirbagheri et al. 2000, Kearney et al. 1997, Zhang et al. 1997, Ludvig et al. 2007, Ludvig & Perreault 2011a].

Limb inertia (I), viscosity (B) and joint stiffness (K) can be identified from the measured joint angle and the torque acting about the joint. This dynamic relationship between the position and the torque can be represented by the following equation:

$$Tq = I\frac{d^2\theta}{dt} + B\frac{d\theta}{dt} + K(t)\theta \tag{2.1}$$

where Tq represents the output torque, θ is the input position of the joint, I is joint inertia, B is the viscosity, and K is the stiffness of the joint. Equation 2.1 is a typical representation of that relation which has been used previously in experimental studies [Popescu et al. 2003, Trumbower et al. 2009].

However, characterising the dynamic behavior of physiological system parametrically can be challenging in experimental conditions and requiring *a priori* knowledge. Another way to characterise a dynamic system is to do so non–parametrically, with its impulse response function (IRF) [Ludvig & Perreault 2011a]. Intrinsic joint stiffness has previously been estimated by means of dynamic IRFs [Kearney et al. 1997, Ludvig & Perreault 2011a]. A systems output can be considered to be a convolution sum of its input and the IRF:

$$y(t) = \sum_{k=0}^{M} h(k)u(t-k) \tag{2.2}$$

where $y(t)$ is the output, $u(t)$ is the input, $h(k)$ is the system's IRF, and M is the number of samples in the system's memory. This represents a *causal* system, where the IRF is a one sided function, depending only on the current and past system inputs. However, dynamic joint stiffness has been represented with two–sided IRF functions, which have non–zero values at negative lags [Westwick & Perreault 2006]. This suggests an *a–causal* system, including an anticipatory element in the model. Rewriting Equation 2.2 into a two–sided discrete convolution yields:

$$y(i) = \Delta t \sum_{j=M_1}^{M_2} h(i,j)u(i-j) \tag{2.3}$$

where $y(i)$ is the output at sample i, $u(i)$ is the input at sample i, $h(j)$ is the IRF, j is the IRF lag, and M_1 and M_2 are the maximum and minimum lags. Even though the IRF can be estimated from data directly, by solving Equation 2.3 for $h(i)$, it is a time and computation intensive process [Ludvig & Perreault 2011b]. As an alternative, the IRF can be found between the position auto–correlation function and the torque–position cross–correlation function [Ludvig & Perreault 2011a]. This results in the following relationship:

$$\phi_{xy}(t,k) = \Delta t \sum_{j=M_1}^{M_2} \phi_{xx}(t-j,k-j)h(t,j) \tag{2.4}$$

where ϕ_{xy} is the torque–position cross–correllation, ϕ_{xx} is the position auto–correlation, and $h(t,j)$ is the time–varying IRF.

Solving Equation 2.4 for $h(t,j)$ yields the following:

$$h(t,j) = \Delta t^{-1}{\Phi_{xx}}^{-1}\phi_{xy} \tag{2.5}$$

where Φ_{xx} is symmetric Toeplitz matrix, and has the following form:

$$\Phi_{xx} = \begin{bmatrix} \phi_{xx}(t-M1,0) & \cdots & \phi_{xx}(t-M2,M1-M2) \\ \vdots & \ddots & \vdots \\ \phi_{xx}(t-M1,M2-M1) & \cdots & \phi_{xx}(t-M2,0) \end{bmatrix} \tag{2.6}$$

and ϕ_{xy} is vector containing the position–torque cross–correlation:

$$\phi_{xy} = \begin{bmatrix} \phi_{xy}(t,M1) & \cdots & \phi_{xy}(t,M) \end{bmatrix} \tag{2.7}$$

Equation 2.5 allows one to calculate stationary and time–varying IRF in an efficient manner. Evaluating the IRFs magnitude along each sample point during a position perturbation gives an estimate of the dynamic joint stiffness [Ludvig & Perreault 2011b].

CHAPTER 3

MOBILE ANKLE AND KNEE PERTURBATOR

The mobile ankle perturbator designed by Andersen & Sinkjaer [1995] is a very useful tool for evaluating the effects of perturbation of the human ankle joint during the complete step cycle of walking on a treadmill [Sinkjær et al. 1996, Sinkjaer et al. 2004].

The device is shown on Figure 3.1 and is an extension of the mobile ankle perturbator presented in Andersen & Sinkjaer [1995]. This mobile ankle and knee perturbator was used to study the electrophysiology and biomechanics during a naturally evoked stretch reflex of the ankle extensors in humans, where a rapid stretch was applied to the ankle joint during walking. The main advantage of this device is that it is capable of delivering perturbations to the ankle or knee joints throughout the entire gait cycle, while maintaining rigid control of the joint without affecting the normal gait pattern.

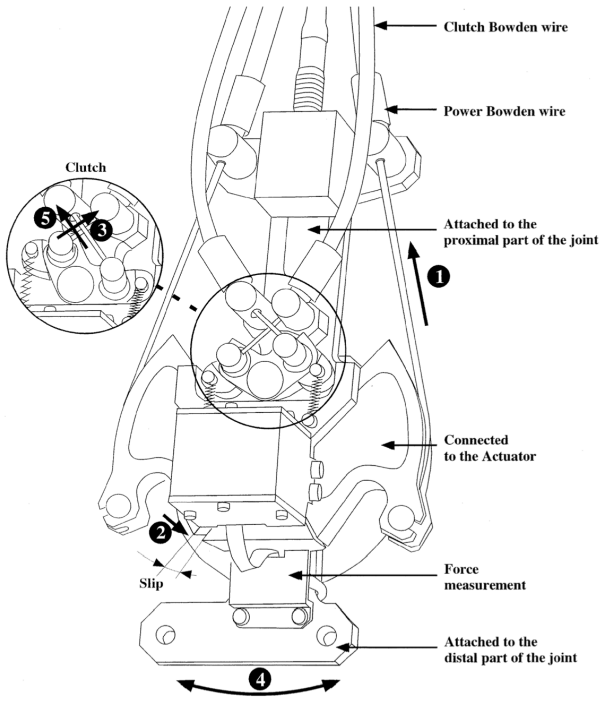

Figure 3.1: The functional joint and the clutch designed by Andersen & Sinkjær [2003], Andersen & Sinkjaer [1995].

The system consist of a mechanical joint, which can be strapped to the calf and the foot of the subject and aligned with the ankle joint, the clutch, the Bowden cables mechanism, the actuator systems, sensors, and the cast. The device is attached to an individual plaster cast of the leg that has to be made for each subject individually, and a carbon fiber-reinforced epoxy

casting to obtain a unique interface from the mechanical joint to the ankle joint. A simplified setup of the device on the ankle joint is shown on Figure 3.2:

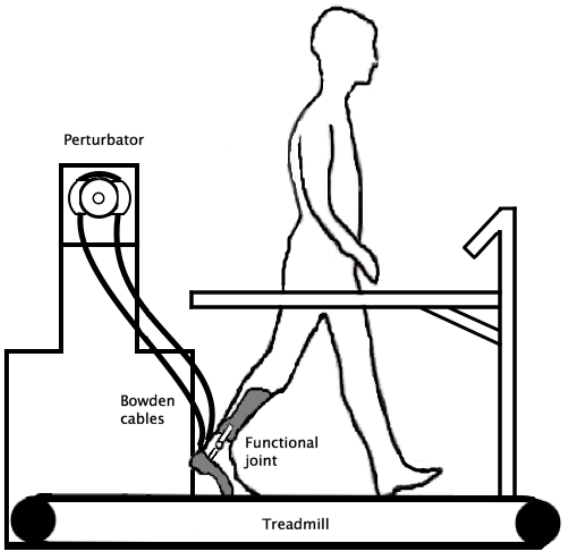

Figure 3.2: The mechanical joint attached to the subject's ankle, connected to the motor placed next to a treadmill by means of Bowden cables.

Functional joint and the clutch

A two–joint system was constructed as means of providing a rigid control. A clutch was incorporated in the mechanical joint that provides a rigid connection when engaged, which is shown in Figure 3.1. Choosing traditional clutch would contribute to an increased weight of the attached system, and this would in turn affect the natural pattern of gait. The system is made of aluminum and its overall weight is 921 grams. The system is based on a two-link mechanical joint aligned on an axis with six independent slide bearings with a clutch mechanism integrated into the functional joint.

The clutch is a two-armed construction; it has ten slide bearings, connected to a double pneumatic cylinder by means of two Bowden wires. When the clutch is disengaged, the arms of the clutch are flexed by two torsion springs, to allow the joint to move within the slip of the two joints. When a perturbation is to be applied, the clutch is engaged. This happens when the actuator pulls the power Bowden wire (as depicted by number **1** on Figure 3.1) causing the slip to be bridged (**2**). This allows space for the clutch to extend its leg by a pull in the Bowden wire of the clutch (**3**). When the leg of the clutch is extended to 180 degrees, the actuator is able to control any rotational movement of the ankle or knee joint by means of the power Bowden wire (**4**). The clutch is released by pulling the second Bowden wire.
The functional joint is shown on Figure 3.3.

Figure 3.3: The functional joint attached to a cast and mounted on subject's left leg.

Bowden mechanism

The two Bowden mechanisms connect the functional joint to the motor and the actuators. The Bowden cable is a a type of flexible cable used to transmit mechanical force or energy by the movement of an inner cable relative to a hollow outer cable housing. The Bowden cable is a flexible, light, and powerful transmission element, and is only able to transmit tensile forces.

Actuator systems

The actuator system consists of a 2.6 kW AC-servomotor, an AC-servo amplifier, and a transmission. This specific combination delivers a rated torque of 100 Nm and a peak torque of 331 Nm of the output shaft of the gear. Andersen & Sinkjær [2003] estimate a power loss of 33% in the Bowden cables, leaving a rated torque of 66 Nm and a peak torque of 222 Nm at the joint. The motor is shown on Figure 3.4.

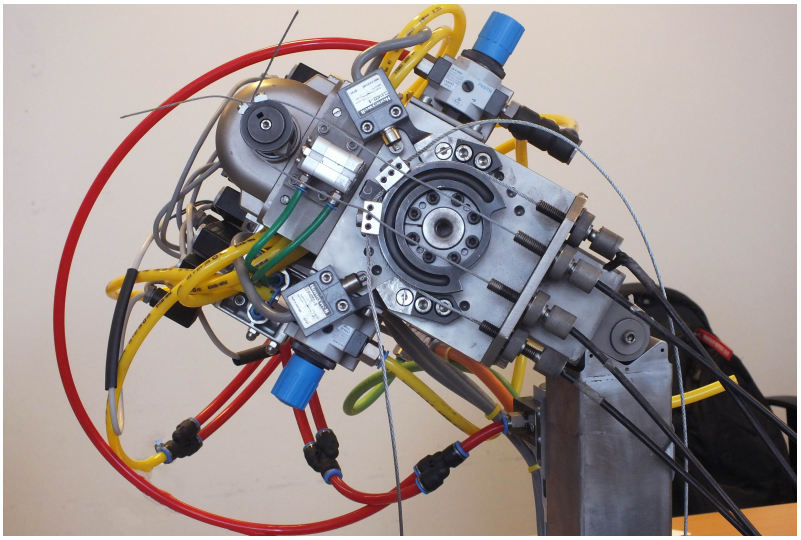

Figure 3.4: The motor of the knee and ankle perturbator.

Sensors

Force measurement sensors is placed proximally on a beam in the part that is attached to the leg. The sensor is a strain–gauge–based force measurement sensor. This sensors allows measurements of torque acting about the joint during a perturbation.

Casting

A carbon–fiber–reinforced epoxy casing is used as an interface between the functional joint and the ankle of the subject to attach the functional joint and align in level with the ankle joint.

CHAPTER 4

AIM OF STUDY

The aim of study was the investigation of ankle stiffness in dynamic conditions of human walking. The focus of the study were the characteristics of ankle joint stiffness in response to perturbations during key phases of the gait cycle. The perturbations of the ankle joint were supplied by a mobile ankle and knee perturbator, which allowed unimpaired gait for the subjects while providing accurate perturbations to the ankle joint. The joint stiffness values were then compared to isometric joint stiffness, obtained from an isometric experiment.

The isometric part of the experiment involved position matching, where the subjects were standing on the treadmill in a posture that corresponded to precise positioning of the legs during these three phases. The three phases of the gait cycle consisted of two phases during the stance and one during the swing phase.

The potential application of this study is in the fields of biomechanics, physiological modeling, and prosthetic and orthotic design. Investigating the stiffness on the ankle joint in dynamic conditions will lead to a better understanding of the muscular and neural control of human joint in motion. This has the potential of aiding the process of rehabilitating or mimicking the function of the joint in response to loss of motor function.

4.1 Hypothesis

It has been demonstrated that the impedance of a human knee during dynamic conditions is much lower than would be predicted from previous isometric studies. This finding recognizes the need for further time-varying approaches in the study of joint impedance. One of the main challenges while investigating joint impedance is that there is no sufficient knowledge about how mechanics of the joints are modulated under different dynamic conditions, for example during gait.

The time–varying estimation of joint stiffness during movement is complicated since the impedance of the joint varies with both the position of the joint and the activation of the surrounding muscles. Therefore, joint impedance during movement depends on two separate time–varying

variables [Mirbagheri et al. 2000, Tai & Robinson 1999, Zhang et al. 1997, Crowninshield et al. 1976]. The study of the stiffness in the human elbow during movements showed that mechanical properties of the joint were time-varying. The stiffness of the arm was found to drop during movement [Bennett et al. 1992].

It can be therefore speculated that the stiffness of the ankle joint measured under dynamic condition also behaves in a time-varying manner and can be speculated to be lower during dynamic conditions than during isometric conditions. Therefore the following hypothesis has been proposed:

The stiffness of the human ankle measured during dynamic conditions such as during locomotion is hypothesised to be lower than stiffness of the ankle joint measured isometrically, during static conditions.

Part II

Solution

CHAPTER 5

EXPERIMENT DESIGN

The experiment setup consists of three main elements: the mobile ankle and knee perturbator (described in detail in Chapter 3), a treadmill and a computer station.

Figure 5.1: The perturbation actuator system.

The actuator system, involving an AC–motor system that is used to provide torque to the mobile perturbator (shown on Figure 5.1), is placed beside the treadmill. By means of Bowden cables the torque of the actuator is transferred to the functional joint attached to the left ankle of the subject.

The functional joint is mounted on casings made of epoxy reinforced with carbon fiber, strapped around the calf and the posterior of the left foot. The two casings which are attached to the calf and the foot of the subject by means of duct tape, with the addition of foam padding (see Figure 5.2). The functional joint was mounted on the casings with the center of rotation (COR) aligned with the left ankle joint. Since making an individual cast of each subject's leg was a time and resource consuming process, pre–made casings of varying sizes are used.

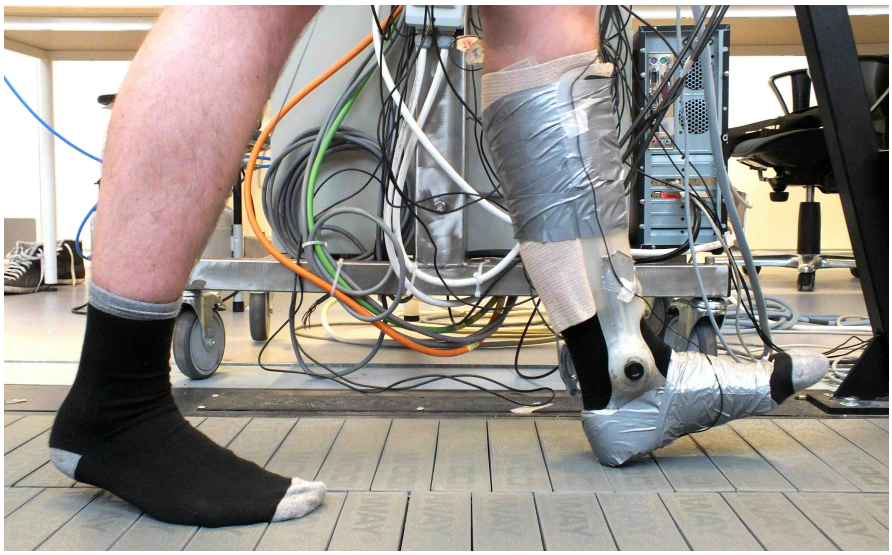

Figure 5.2: The casing attached to the subject's leg while walking on the treadmill.

The treadmill used was a split–belt treadmill (Woodway USA, Inc.), with speed controls, adjustable hand rails and a safety stop; however, the split–belt functionality was not used in this project.

The computer station was used to run the software used to control the experiment as well as collect data. The main piece of software used was the Mr. Kick, developed at Center for Sensory-Motor Interaction (SMI), Aalborg University, Denmark, which collects and, if needed, pre–processes the experiment data. Additionally, a program was used for treadmill control. Mr. Kick software was used to collect the data recorded during the experiment, which include:

- Electromyograph (EMG) data from soleus and tibialis anterior muscles
- Angular joint position of the ankle joint
- Torque around the ankle joint
- Heel trigger data

EMG data were collected using bipolar surface electrodes placed 0.5 cm apart on the soleus (SOL) and the tibialis anterior (TA) muscles of the left leg, and pre–amplified before being fed into an EMG amplifier rack. A ground electrode was placed on the kneecap. A force sensitive resistor (FSR) was placed under the heel of the subject and taped in place underneath the heel–cast. The heel trigger data were fed into a separate amplifier on the data collecting rack and sent to Mr. Kick together with the EMG data. Angular position, torque, and surface EMGs from SOL and TA were sampled at 4 kHz by a analog-digital converter (ADC) in sweeps of 2 seconds each. The torque and angle data from the mobile perturbator were fed directly into the computer from a computer station used by the mobile perturbator, via an ethernet cable. The EMG's were pre-amplified and fed to PC equipped with a data collection module (Data Acquisition Card PCL718).

5.1 Perturbations

The aim of the perturbation was to cause a change in angular position of the joint, which will be translated into torque by the structures around the joint. The perturbation specifications are set to impose a change in position significant enough to allow the calculation of the joint stiffness, but not large enough to destabilise the posture of the subject. All perturbations were applied once every 5 to 10 steps. This allowed the subject to recover from the perturbations and disallowed the subjects to anticipate and prepare for perturbations by co–contracting muscles around the ankle joint. There was a single displacement pulse during a gait cycle, with specifications based on those used by Andersen & Sinkjaer [1995], which are outlined in Table 5.1 and shown in Figure 5.3. The perturbator system operates in degrees, but for the purpose of further analysis the position angle was converted into radians. Hence, the perturbation amplitude of 8° is later referred to as 0.140rad.

Parameter	Value
Amplitude	8°
Velocity	$300°/s$
Hold time	$200ms$

Table 5.1: Perturbation parameters used.

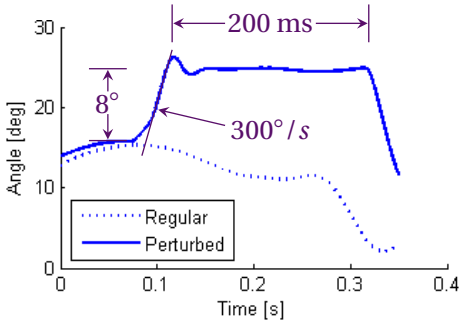

Figure 5.3: Example of a single perturbation, compared to a regular, non–perturbed signal (dotted line). Perturbations parameters are shown.

In order to be able to measure joint characteristics during the whole gait cycle, the perturbations were spread over both the stance and swing phases. The joint was perturbed in three periods of the gait cycle: two during the stance phase and one during the swing phase. The stance perturbations were applied during the midstance period, at 20% of stride length and at transition between heel off and pre–swing, at 50% of stride length. The swing perturbation was applied during deceleration period, at 90% of stride duration. The perturbations were dorsi– and plantarflexions. The order in which the perturbations were applied in was randomised.

5.1.1 EMG data

The EMG data will be collected from the main dorsiflexor muscle, the tibialis anterior (TA) and a plantarflexor, the soleus muscle (SOL). The soleus muscle was chosen for recording based on the fact, that it is the only muscle in the triceps surae group that is not biarticulate, and only articulates the ankle joint. The EMG's will be recorded with bipolar surface electrodes, pre–amplified and fed to PC (info on the PC) equipped with a data collection module (Data Acquisition Card PCL718) at a sampling rate of 4 kHz.

5.2 Procedure

Preparing each experiment started with assembling all necessary materials and tools around the treadmill. Before the experiments started, the area in each subject's lower leg was shaven for electrode placement, the electrodes were placed and the leads attached to the electrodes. Once that was done, the subject was asked to do a series of contractions of the muscles while standing to assess the precision of the electrode placement.

With the previous steps done, the functional joint was put onto the subject. This was done using a chair positioned close by or on the treadmill itself, as it requires the subject to safely put the cast with the functional joint on. The heel switch was placed under the heel portion of the foot casing. Once the cast was positioned and fastened in place with duct tape, all leads (EMG and heel contact) were finally attached for data collection.

5.3 Experiment protocol

Once the subject was prepared, all the equipment was safely and comfortably put on, the experiment could start. The ankle joint stiffness was investigated during both dynamic and isometric conditions. The purpose of the dynamic part of the experiment was to investigate the modulation of ankle joint stiffness in human walking. The purpose of the isometric part was to measure the ankle joint stiffness in response to perturbations during static conditions, and to compare these two conditions. The isometric part of the experiment focused on position matching, where the subject was standing on the treadmill in a manner that was matching the three periods of the gait cycle. The perturbations were applied to the left ankle, while the subject was standing with his/her legs placed on the treadmill in a way that corresponded to positioning of the legs at the precise moments of 20%, 50%, and at 90% of stride duration.

The order in which the experiment was carried out was randomised, i.e. it was determined at random, whether the dynamic part was performed first, or the isometric.

Leg positioning procedure

In order to be able to determine where the subject needed to place their legs during the isometric part, the experiment started with determining the exact spots on the treadmill that corresponded to the spots on which the legs would be placed during walking precisely at 20%, 50%, and at 90% of the gait cycle. This was necessary if the isometric experiment was to take place first. In order to do that, the cast was put on the subject's ankle (however, without the functional joint attached to it) and secured to the calf with a velcro. Secondly, the subject was asked to step onto the treadmill and find a comfortable walking speed (usually around 4 km/h). Simultaneously, a camera was placed next to the treadmill, and when the subject was walking, the gait pattern was recorded on video. Once this was achieved, the subject would step down from the treadmill and the electrode placement process would begin, while at the same time, the other group member processed the video and extracted one gait cycle from it. Then, a number of frames in that video was calculated in a MATLAB script, and three images were obtained, which showed the placement of the subject's leg at 20%, 50%, and at 90% of the gait cycle (which corresponded to 20%, 50%, and at 90% of frames in that one gait cycle video). A measuring tape had been glued to the floor right next to the treadmill to serve as guidings

markings, so the positioning of the legs could be recreated from the three pictures. An example of the final positioning at those three spots is shown on Figure 5.4.

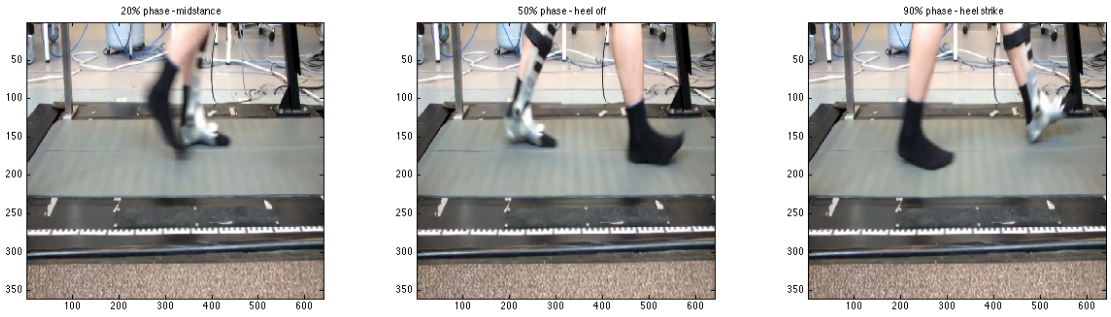

Figure 5.4: The positioning of the legs during 20%, 50%, and at 90% of the gait cycle, with the guidings markings measure placed next to the treadmill.

Measuring gait pattern

The dynamic part of the experiment started with the perturbator system in passive mode, in order to collect information about the gait pattern of each subject. The task of the functional joint in the passive mode was to follow the movement of the ankle without interfering or changing the natural gait pattern. The subject was asked to walk on the treadmill, so he/she can get adjusted to the presence of the functional joint on their lower leg, and to walking with it on the treadmill. Then, a comfortable walking speed needed to be found by the subject and once the subject was adapted to the experience of the functional joint, 20 step cycles are recorded. This, combined with data from the heel switch, allows finding the precise timing of gait pattern phases. When 20 step cycles were recorded, the average stride duration was extracted and then used to time the perturbations. The joint needs to be perturbed in the following periods of the normalized step cycle: at 20% of stride duration, at 50%, and at 90% of stride duration.

5.3.1 Dynamic experiment

The kinematics of the human ankle joint were investigated during gait at a comfortable walking speed preferred by the subject (around 3.9 km/h). Once the gait pattern duration has been measured, the dynamic part of the experiment can start. The task of the active mode was to transfer a rotation from the actuator to the ankle joint to impose a stretch of the ankle extensors or flexors, i.e. cause a perturbation of the ankle joint. The perturbations were done with the specifications listed on page 35, and applied at the three previously described timings for both plantarflexion and dorsiflexion, resulting in the dynamic experiment consisting of six parts, listed below:

- 20% plantarflexion
- 20% dorsiflexion
- 50% plantarflexion
- 50% dorsiflexion
- 90% plantarflexion
- 90% dorsiflexion

The order in which these perturbation–timings were applied was randomised. The order in which the different timings was chosen at random for all subjects (i.e. the order of the 20%, 50%, 90% stride durations), and the order in which plantarflexion and dorsiflexion was chosen was also random between the subjects as well.

After the dynamic part of the experiment was finished, and all the three timings for both plantarflexion and dorsiflexion were performed, the subject was given a short break before the isometric part of the experiment began. The subject was asked to step away from the treadmill and moved (together with the entire perturbation system) to a chair situated next to the treadmill for the isometric, sitting part of the experiment.

5.3.2 Isometric experiment

During the isometric part of the experiment, the subjects were instructed to stand still in positions mimicking the respective three phases of gait that were also examined in the dynamic part of the experiment.

As described previously, to provide a precise frame of reference, the subject's gait was recorded with a video camera during the 20 strides used to acquire the gait pattern characteristics. A ruler was placed along the entire side of the treadmill. The recording was then analysed in Matlab to find the exact position of each foot and the distance between them during the three phases of gait. The subjects were then guided to stand while maintaining the position. The positions were then copied onto the treadmill, so that the position of each foot during the three phases could be found and kept easily. Additionally, the subjects were allowed to hold on to a railing while they were maintaining the poses, as it was evaluated that the effect on the dynamics of the ankle joint would be minimal, while it would provide the necessary stability.

The positions examined were closest approximations of conditions during the dynamic experiment. Positions were approximated at 20%, 50%and 90% of gait. At each of the positions, the ankle was perturbed by means of a plantar– and dorsiflexion, each perturbation repeated 20 times. During the isometric experiments, the same sets of data were measured, as during the dynamic experiments: EMG from TA and SOL, torque and ankle data. Heel trigger data was not used during this part, but as the order of experiments was randomised, the heel trigger was still placed under the subject's heel when the mobile perturbator cast was put on.

The perturbations were also done with the same specifications as for the dynamic part, listed on page 35, and applied at the three previously described timings for both plantarflexion and dorsiflexion, resulting in the isometric experiment also consisting of six parts:

- 20% plantarflexion
- 20% dorsiflexion
- 50% plantarflexion
- 50% dorsiflexion
- 90% plantarflexion
- 90% dorsiflexion

The order in which these perturbation–timings were applied was also randomised between the subjects, as well as the order in which plantarflexion and dorsiflexion was chosen.

CHAPTER 6

DATA ANALYSIS

The following chapter contains the description of data processing and analysis techniques, that allowed the extraction of joint stiffness results from the collected data.

6.1 Data collection

In the course of the experiments, data were collected from 11 healthy subjects (9 males and 2 females, with an age range of 24-27 years). The data collected were:

- EMG from TA and SOL muscles
- Joint angle data
- Torque around the ankle joint
- Heel trigger data

The data were collected with a sampling frequency of 4000 Hz, in separate, 2s sweeps. The sampling of the 2s sweeps was initiated using the heel trigger, at heel strike of the left foot. The EMG data were filtered upon recording, with a second order, bandpass Butterworth filter, with a high pass cutoff frequency of 10 Hz and a low pass cutoff of 500 Hz.

Each perturbation combination (as described in section 5.3) was collected in 20 repetitions, apart from cases, where incorrect sweeps were detected (in cases where a safety limit was triggered, or the subject stepped incorrectly), when additional repetitions were recorded, to a total of 20 correct sweeps. During the dynamic experiments, for each sweep of perturbation during walking, a sweep without a perturbation was recorded to serve as a control trial as well as to monitor the subjects' stride duration during the dynamic experiments.

6.2 Data processing

After the data were collected and stored on a PC, they were processed in a series of steps in order to extract the joint stiffness information. The first step, that was done was screening the

data for incorrect sweeps and removing them from further analysis. The incorrect sweeps were mostly caused by the perturbation being interrupted by activation of the motor safety limits, or the subjects stepping incorrectly, due to temporary loss of balance, and resulted in either the perturbation not achieving the necessary amplitude or causing the gait profile to differ significantly from the mean gait cycle profile.

Once the data were screened, the sampling frequency was reduced to remove redundant data and make the analysis process faster. This was done using Matlab's `decimate` function, and the data were resampled at 1000 Hz. Even though the data were collected in two second sweeps, where the acquisition always started at left foot's heel strike, additional alignment was necessary in order to ensure, that data segments from separate subjects were analysed over the same time with respect to the perturbation. This was a means of ensuring that the time–varying behavior could be assumed to be the same across the multiple realisations of data.

To align the position and torque data, windowed data segments were extracted from the 2s sweeps, starting from the perturbation onset, which was recorded for every single perturbation sweep. A window of 300 ms was used, which was enough to include all data points carrying information related to the perturbation.

After the collected data were screened for bad sweeps, correctly aligned and windowed, the stiffness values could be calculated.

6.3 Stiffness calculation

The first step in calculating the stiffness was removing the mean offset from both the position and torque data to center them around zero. Dynamic joint stiffness was then calculated by finding the time–varying IRFs, by implementing Equation 2.5. The IRFs were calculated with 4 lags on either side of the middle point.

The input auto–correlation (Φ_{xx} in Equation 2.5) was found using the position data, and pinput–output cross–correlations (ϕ_{xy} in Equation 2.5) were found using the position data as input and torque data as output. Then a singular value decomposition (SVD) pseudoinverse was found for ${\Phi_{xx}}^{-1}$ from Equation 2.5. Using SVD gave the following:

$$\Phi_{xx}(i) = \mathbf{U}(i)\mathbf{S}(i)\mathbf{V}(i)^T \tag{6.1}$$

where $\mathbf{S}(i)$ is a square matrix, whose diagonal elements are singular values of $\Phi_{xx}(i)$, and $\mathbf{U}(i)$ and $\mathbf{V}(i)$ are unitary matrices. With these elements, the inverse of Φ_{xx} could be expressed as:

$$\Phi_{xx}(i)^{-1} = \mathbf{U}(i)\mathbf{S}(i)^{-1}\mathbf{V}(i)^T \tag{6.2}$$

Once the IRF values could be found for every point in the 300 ms window, the dynamic stiffness values were calculated by finding the area under the graph of the absolute value of the IRFs.

6.3.1 Method assumptions

A number of assumptions were made during application of the methods described in the above sections.

It was assumed that the system varied with time in the same way for all repetitions of each specific perturbation. This meant that data from repetitions of specific perturbation combination form an ensemble of multiple short data segments. This assumption implied short–time stationarity of data (quasi-stationarity) across the ensemble of multiple data segments [Kirsch et al. 1992, Ludvig & Perreault 2011b].

It was also assumed that the dynamic changes of the ankle joint system can be characterised using two–sided IRFs [Westwick & Perreault 2006].

CHAPTER 7

RESULTS

During dynamic conditions of walking the stiffness of the ankle joint after an imposed perturbation is speculated to depend on the phase of the gait cycle in which a perturbation is applied to the joint, and/or the direction of the imposed perturbation (plantarflexion and dorsiflexion). To investigate the influence of these factors, the angular displacement of the ankle joint and the resulting torque response was studied at different times in a step at a fixed walking speed. Additionally, the angular ankle joint displacement evoked by a perturbation and the resulting torque response was investigated in static conditions.

7.1 Dynamic experiment

The ankle joint stiffness was investigated during dynamic conditions to examine the stiffness modulation during three phases of gait cycle: at 20%, 50%, and 90% of the gait cycle duration, with perturbations in both the dorsiflexion and plantarflexion directions.

Subjects walked on the treadmill with a comfortable walking speed chosen by each subject, while the data from the heel switch allowed calculating the precise duration of each subject's gait. The average stride duration was extracted to calculate precisely when in the gait cycle the perturbations needed to be applied. The walking speeds for each subject are shown on Table 7.1. The mean walking speed for 11 subjects participating in the experiment was 3.84 km/h, with a standard deviation of 0.146 km/h.

The mean durations of the gait cycles are also shown on Table 7.1, with standard deviations for each gait cycle durations. The values of the mean and standard deviation were calculated from five recorded values of gait cycle duration for each subject.

The length of the stride for each subject was monitored during the experiment, in order to ensure that the stride duration did not change considerably during the length of the experiment. If that happened to be the case, it could possibly result in an incorrect perturbation-application timing. The gait cycle length was checked manually multiple times during the dynamic part of the experiment, and the duration was calculated.

Subject .:	Walking speed [km/h]	Mean gait cycle duration [s]	Standard deviation [s]
1	3.80	1.150	0.010
2	3.90	1.096	0.015
3	3.83	1.216	0.010
4	3.95	1.078	0.015
5	3.80	1.147	0.025
6	3.80	1.096	0.025
7	3.65	1.089	0.008
8	4.05	1.120	0.007
9	3.65	1.282	0.019
10	4.10	1.156	0.053
11	3.75	1.252	0.008

Table 7.1: The walking speeds for the 11 subjects participating in the experiment, with the average values of the gait cycle durations and the corresponding standard deviations.

The recorded values of the gait cycle durations are shown in section A.1 of the Appendix (Table A.1, page 71), where each individual gait cycle duration of each subject is documented during the duration of the dynamic experiment.

The use of a metronome to help the subjects maintain the rhythm of walking with constant speed proved to be an effective solution. Maintaining a constant stride duration ensured that the recordings were only made for comparable steps, and the perturbations were applied at the correct time of the gait cycle. The recorded average gait cycle durations of each subject shown on Table 7.1 differed moderately in-between the subjects, since every subject chose their own walking speed. The standard deviations ranged between the lowest SD of 0.007 s for subject 8, and highest SD of 0.053 s for subject 10. In statistics, standard deviation represents how much variation there is from the average value. Since the standard variations calculated for all the 11 subjects were within the range of 8-53 milliseconds, these standard deviations indicate that the data points were very close to the mean value of the gait cycle durations.

Figure 7.1 shows the graphical representation of the changes in gait cycle duration (represented in seconds on the y-axis) throughout the duration of the dynamic experiment (represented in minutes on the x-axis, where 0 min represents the initiation of the experiment).

Two subjects are shown on the figure, both as data points and a best fit line. Even though none of the subjects had any considerable deviations from the mean gait cycle duration, Figure 7.1 shows how the length of the gait cycle fluctuated during the experiment. Subjects 6 (shown in red) and 8 (shown in blue) are represented as examples of the altering and non-altering gait durations cases respectively.

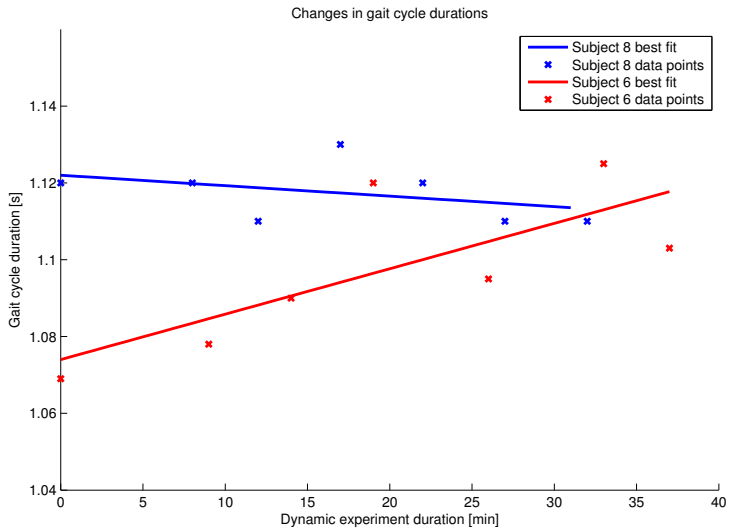

Figure 7.1: The gait cycle durations of two subjects with gait cycle duration–altering and non-altering tendencies throughout experiment respectively.

For these two subjects, seven data points were recorded and plotted on the figure, and a best–fit line was added to show the tendency of the durations to either elongate, shorten or remain constant. The best–fit line serves to show, if a subject managed to maintain the same gait duration throughout the dynamic experiment, or his/her gait duration had a tendency to deviate.

Subject 8 showed an almost constant gait cycle duration for the entire span of the dynamic experiment (32 minutes). Subject 6, despite not having the highest standard deviation of the gait duration, showed a clear tendency of elongation of the gait duration in the course of the dynamic experiment (37 minutes). Even though subject 6 exhibited an increasing trend to elongate the gait cycle during experiment, the deviation from the mean gait cycle duration was almost negligible. All other subjects exhibited no major duration deviations.

7.1.1 Perturbations imposed during walking

A perturbation of 8° (0.140 rad) with a velocity of 300°/*s* and with a hold time of 200 ms was applied at a rate of one perturbation for every 5 to 10 steps, until 20 position and torque perturbation–responses were collected for each subject. The applied perturbations were both in dorsiflexion and plantarflexion directions. When applied, they caused a displacement of the ankle joint angle and caused a significant torque response.

Figure 7.2 shows the averaged position of the ankle joint with and without a perturbation in mid-stance in one subject walking at 3.80 km/h, the resulting averaged torque for the perturbation and the EMG activity of the Tibialis Anterior (TA) and Soleus (SOL) muscles.

Each graph shows superimposed average responses with control steps (blue lines) and steps in which a perturbation was applied (green lines). All data for both plantarflexion and dorsiflexion are averaged over n=20 measurements. Graphs on the left side show the average *plantarflexion* perturbation applied to the ankle joint during the dynamic experiment at the 20% of the gait cycle, and graphs on the right show *dorsiflexion*. The vertical red dashed line

corresponds to the perturbation application timing of 20% of the gait cycle duration, and the beginning of the gait cycle (at time 0 s) began with heel contact.

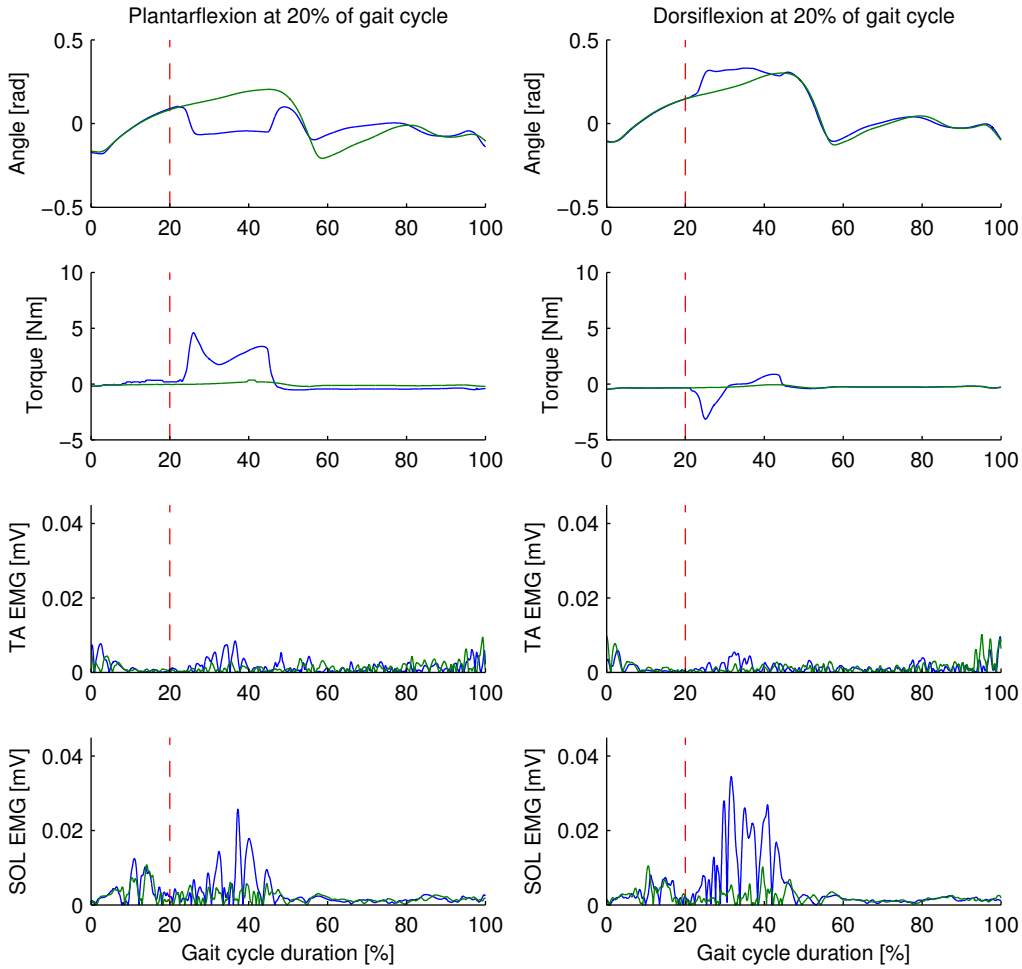

Figure 7.2: Averaged (n=20) position of the ankle joint with and without a perturbation during walking shown with the resulting averaged torque for the perturbation and the EMG activity of TA and SOL – example of a typical subject during plantar flexion at 20% of the gait cycle duration during stance phase. Subject 1.

A change in the angle of the joint, the corresponding torque acting about the joint during the perturbation, and the EMG activities of the TA and SOL muscles are shown when a perturbation was applied at the 20% of the gait cycle duration, which corresponded to 0.230 seconds of the gait cycle in that particular subject (20% of a 1.15s gait cycle, Subject 1). The steps in which a displacement was imposed deflected visibly from the position of the control steps by a 0.140 rad displacement. All the graphs show the mean values for the angle, torque and EMG signals (perturbed and unperturbed) for a typical subject, i.e. the average of all the sweeps with and without perturbations.

The plantarflexion perturbation (Fig. 7.2, *left*) applied at time 20% was reflected in an increase in torque, with a peak amplitude of 4.5 Nm. During the initial the torque was dominated by the inertia and the intrinsic properties of the muscle–tendon complex around the joint [Sinkjaer et al. 1988]. The decline, which followed the peak torque, was caused by a decrease in in the

velocity of perturbation, while the following additional increase in torque starting about 115 ms after perturbation initiation onset (10% of gait duration after perturbation) was believed to be a result of the SOL stretch reflex [Sinkjær et al. 1996].

There was observed a spike in SOL EMG activity during both plantarflexion (Fig. 7.2, *left*) and dorsiflexion, (Fig. 7.2, *right*), where a SOL stretch reflex occurred approximately at 30% of the gait cycle duration (170 ms after perturbation initiation). When the perturbation was released after 200ms of hold time, the torque returned to the same value as during the control step (0 Nm). The EMG activity of SOL during dorsiflexion reached 0.035 mV in its peak value and lasted the entire duration of the perturbation hold time (200 ms), as SOL was stretched during that phase of the gait cycle. In comparison, the SOL peak amplitude during plantarflexion was lower (max. amplitude of approximately 0.025 mV).

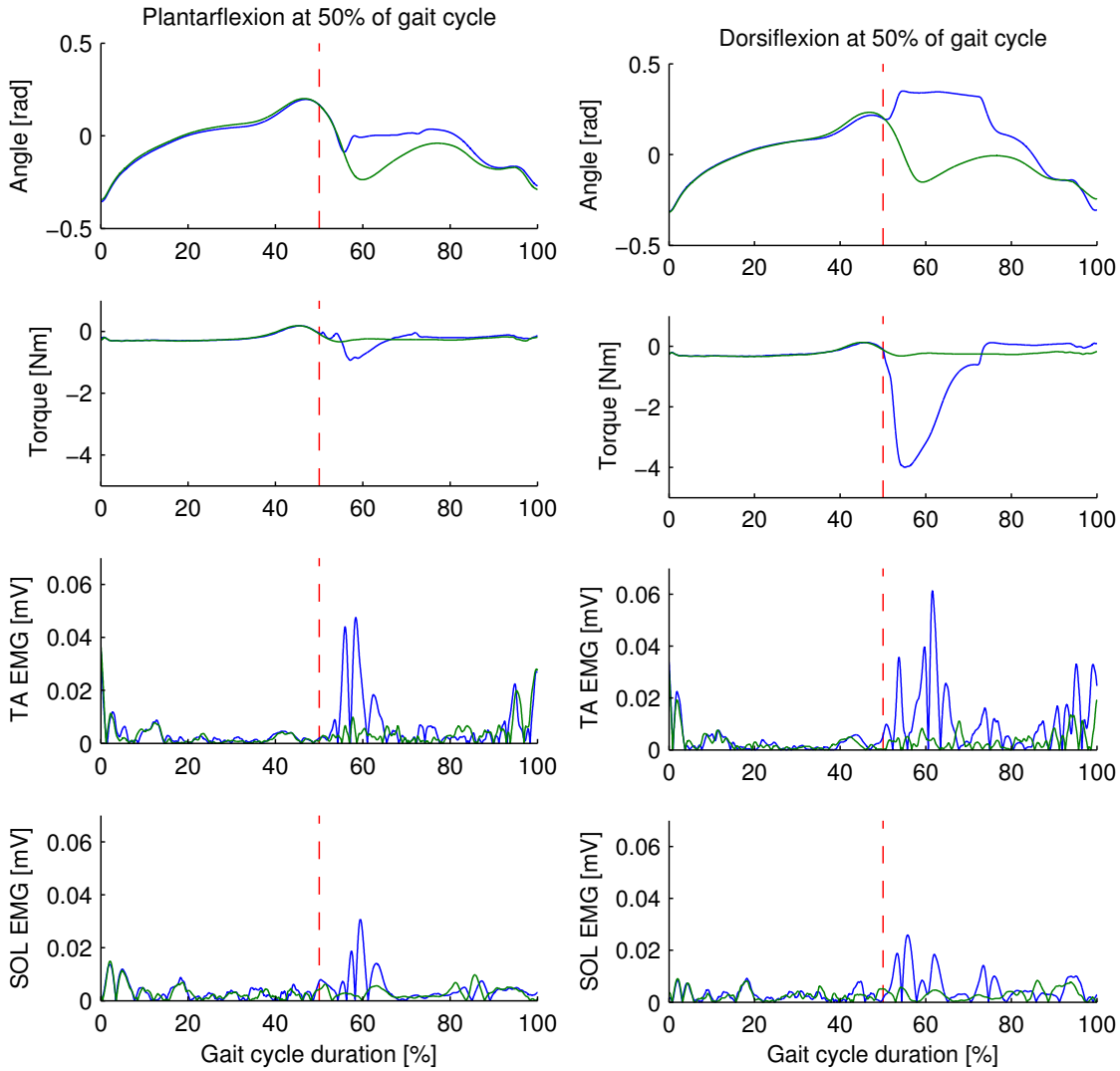

Figure 7.3: Averaged (n=20) position of the ankle joint with and without a perturbation during walking shown with the resulting averaged (n=20) torque for the perturbation and the averaged (n=20) EMG activity of the TA and Soleus muscles. The example of a typical subject during plantar flexion at 50% of the gait cycle duration during the stance phase. Subject 8.

Figure 7.3 shows the average position of the ankle joint with and without a perturbation during walking, the resulting average torque and EMG activity of TA and SOL muscles. Graph on the left side shows the *plantarflexion* perturbation applied to the joint during the dynamic experiment at the 50% of the gait cycle. All data for the plantarflexion was averaged over n=19 measurements. Graph on the right shows a *dorsiflexion*, where all data was also averaged over n=20 measurements. The difference in the number of measurements was caused by a necessity to discard one sweep from the plantarflexion measurement. Once more, the vertical red dashed line corresponds to the perturbation application timing of 50% of the gait cycle duration. Similarly, the blue signal on all graphs is unperturbed, and the green is perturbed.

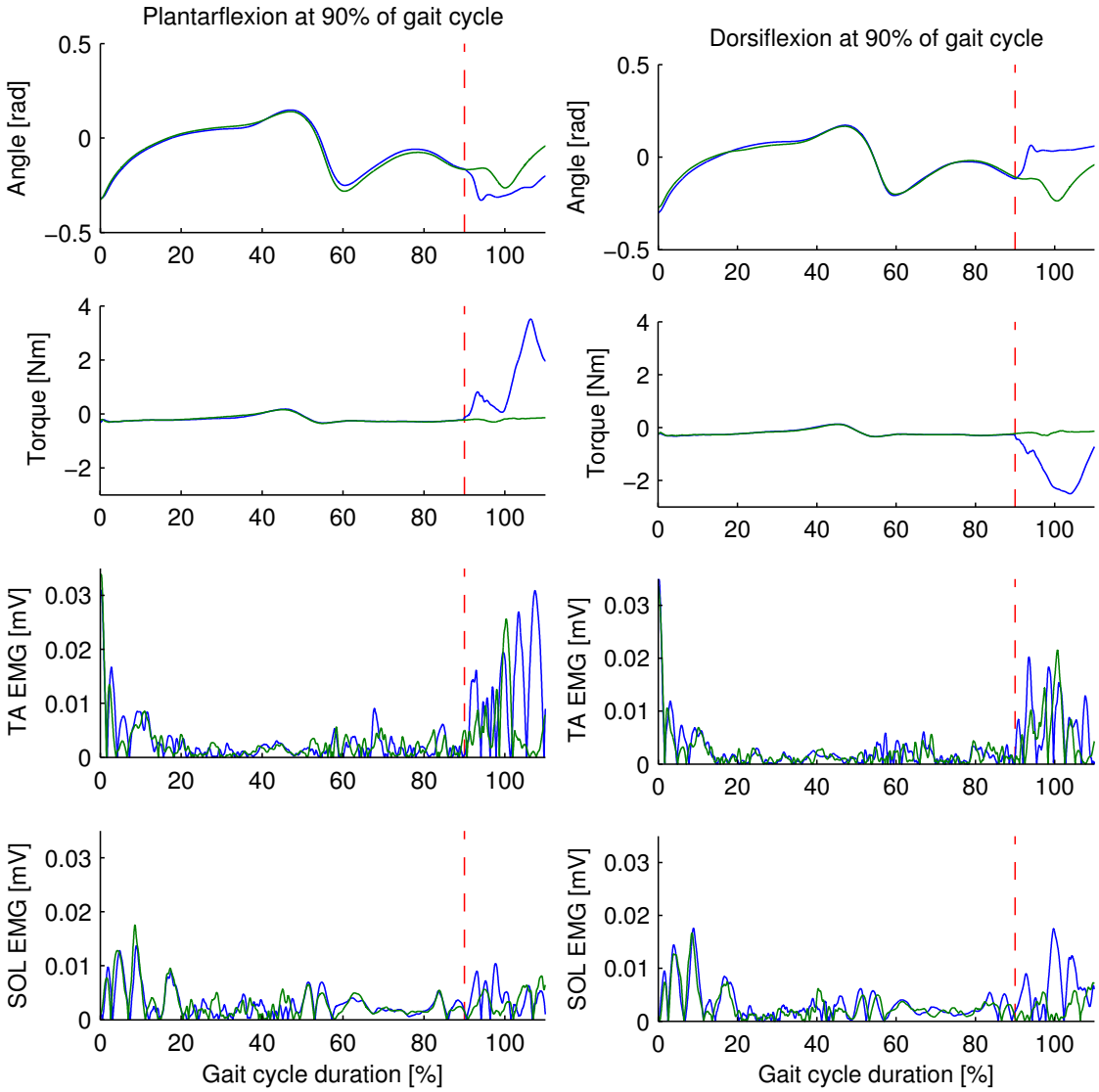

Figure 7.4: Averaged (n=20) position of the ankle joint with and without a perturbation during walking shown with the resulting averaged (n=20) torque for the perturbation and the averaged (n=20) EMG of TA and SOL. The example of a typical subject during plantar flexion at 90% of the gait cycle duration during the swing phase.

Figure 7.4 shows the average position of the ankle joint with and without a perturbation during

walking, the resulting, torque and the EMG activity of TA and SOL during the dynamic experiment at the 90% of the gait cycle. All data was averaged over 20 measurements. Graph on the left side shows the average *plantarflexion* perturbation applied to the joint, and graph on the right shows a *dorsiflexion*. The vertical red, dashed line corresponds to the perturbation application timing of 90% of the gait cycle duration. Figure 7.4 shows 110% of the gait cycle duration (i.e. one entire gait cycle and the beginning of another), since that particular perturbation–timing occurred late in the cycle and therefore would not be clearly visible on the figure.

There was observed an increased activity in TA EMG during both plantarflexion (Fig. 7.4, *left*) and dorsiflexion, (*right*), where a TA stretch reflex occurred. The EMG activity of TA during plantarflexion reached 0.035 mV in its peak value and lasted the entire duration of the perturbation hold time (200 ms), as TA was stretched during that phase of the gait cycle during a plantarflexion perturbation. That direction of perturbation caused the TA to stretch, while SOL was unloaded at that moment.

The EMG activity of SOL was more more pronounced during dorsiflexion (7.4, *right*), since SOL was stretched as a result of a dorsiflexion perturbation at that phase of the gait cycle.The EMG activity of both muscles reached the same maximal amplitudes both during the unperturbed and perturbed steps.

7.2 Isometric experiment

7.2.1 Perturbations imposed during standing

The perturbations during the isometric experiment were applied to the ankle joint, when the subjects were instructed to stand still in postures mimicking the respective three phases of gait, which were the closest approximations of conditions during the dynamic experiment (postures approximated at 20%, 50% and 90% of the gait cycle).

At each of the positions, the ankle was perturbed by means of a plantar– and dorsiflexion, each perturbation repeated 20 times. Since the perturbations were applied during isometric conditions, the subjects were stationary on the treadmill, and therefore perturbations were applied at the beginning of each sweep and did not occur at other different timings. This is visible on both figures 7.5 and 7.6, where the perturbations occur at the same timing of 0.2 seconds. Figures 7.5 and 7.6 show an example of the changes in ankle joint angles, torques, and TA and SOL EMGs in plantarflexion and dorsiflexion directions respectively.

Figure 7.5 shows the position of the joint and torque as a response to a perturbation that occurred when a subject was standing in a posture that corresponded to 20% of the gait cycle duration, and the perturbation was applied in the plantarflexion direction. Joint angle and torque values for the remaining measurements at postures of 50% and 90% of the gait cycle duration have a very similar appearance and are therefore not shown on additional figures.

The TA EMG activity during a plantarflexion perturbation (Fig. 7.5) shows the average stretch reflex, while there is no visible EMG activity other than the background EMG. The perturbation during the 20% of the gait cycle occur when the subject's body weight is entirely on the left leg, and the plantarflexion perturbation forces the foot downwards towards the ground, and thus causes a tendency to lift the body upwards. This is visible in the EMG activity of TA, which is

stretched during that perturbation.

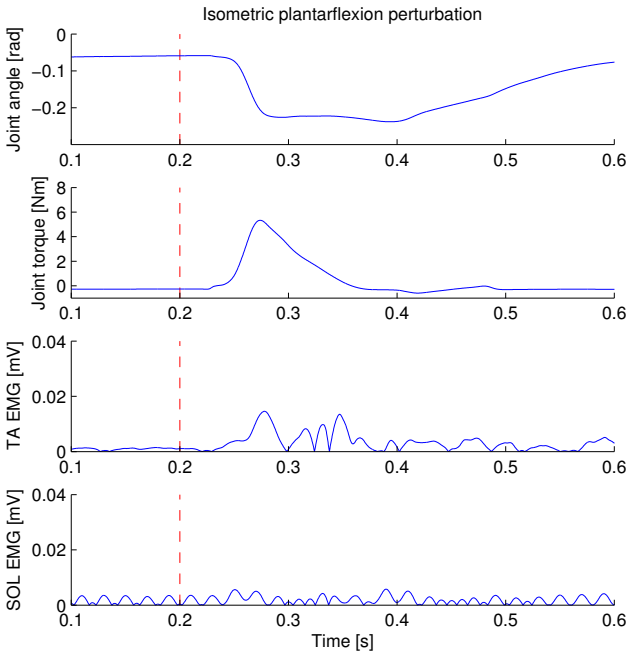

Figure 7.5: An isometric plantarflexion perturbation of a typical subject maintaining the posture corresponding to leg placement during 20% of the gait cycle duration in the dynamic part of the experiment, with a plantarflexion perturbation. Subject 3.

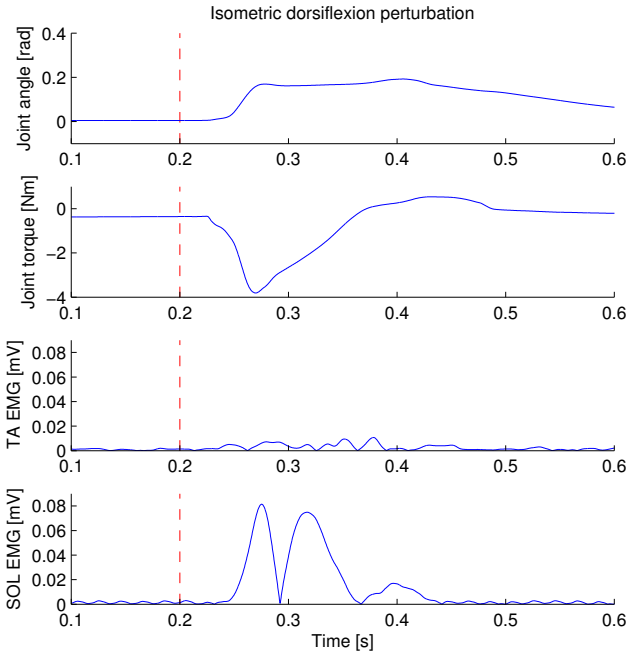

Figure 7.6: An isometric dorsiflexion perturbation of a typical subject maintaining the posture corresponding to leg placement during 20% of the gait cycle duration in the dynamic part of the experiment; a dorsiflexion perturbation. Subject 3.

The TA EMG activity during a plantarflexion perturbation (Fig. 7.6) was in turn minimal during the dorsiflexion. The perturbation caused the foot to move upwards, and since the body weight did not counteract that movement, the stretch reflex in SOL was more pronounced, with the amplitude of over 0.08 mV. This is visible in the EMG activity of SOL, which was stretched during that perturbation, while TA remained inactive.

7.3 Ankle stiffness modulation

The purpose of the dynamic and isometric experiments was an investigation of ankle stiffness modulation measured in both dynamic and isometric conditions, and a comparison between the two conditions in three phases of the gait cycle. For that reason, the ankle joint modulation was first analysed between the dynamic and isometric conditions. Secondly, stiffness modulation between the three phases of gait cycle was analysed.

7.3.1 Statistical analysis

The collected data were analysed by means of a two–factor analysis of variance (ANOVA), which is described in detail in section A.2 of the Appendix, on page 72. The two examined factors were factor A: dynamic or isometric measurement, and factor B: phases of gait cycle (20%, 50%, and 90% of gait cycle duration).

The two-factor ANOVA performed on the data showed that there was a statistically significant difference in mean ankle stiffness between the three phases of gait cycle during the plantarflexion measurements only (i.e. $\mu_{20\%}, \mu_{50\%}, \mu_{90\%}$ were not the same, where μ is a mean of the ankle stiffness) [$P < 0.0005$]. Additionally, a Tukey HSD *post-hoc* analysis showed that the individual mean stiffness values during the three phases of the gait cycle in plantarflexion experiments were all different (detailed results shown in section A.3 Appendix, page 75).

7.3.2 Dynamic and isometric comparison at 20% of the gait cycle

Figure 7.7 shows a comparison of the angular position and torque data, averaged across repeated sweeps of individual subjects (n=20), and across all subjects (n=11), as well as modulation of the ankle joint stiffness during walking 20% of gait cycle in plantarflexion direction (*left*) and dorsiflexion (*right*). Figure 7.7 shows the period between the onset of perturbation until after the end of the hold time. Predominantly, stiffness appeared to fluctuate during these two moments, namely the initialization of perturbation, and the release of the hold.

The mean values of stiffness in both dynamic and isometric trials were non-significantly different (two-factor ANOVA, [P = 0.77383]). However, the values of stiffness have been observed to vary between the dynamic and isometric trials at 20% of the gait cycle duration. At the initial phase of the perturbation during *plantarflexion* (t = 41 ms) (Fig. 7.7, *left*), the maximum peak isometric stiffness was 1283 ± 1029 Nm/rad, whereas at the same timing during the dynamic trial, maximum mean stiffness was 707 ± 802 Nm/rad. During the hold-release time, both the isometric and dynamic stiffness values were within a close range of each other (859 ± 519 Nm/rad isometric at t = 266ms, and 877 ± 678 Nm/rad dynamic t = 274ms).

Similarly, during *dorsiflexion* (Fig. 7.7, *right*), at the initial phase of the perturbation (t = 42 ms) the maximum peak isometric stiffness was 405 ± 337 Nm/rad, whereas at the same timing

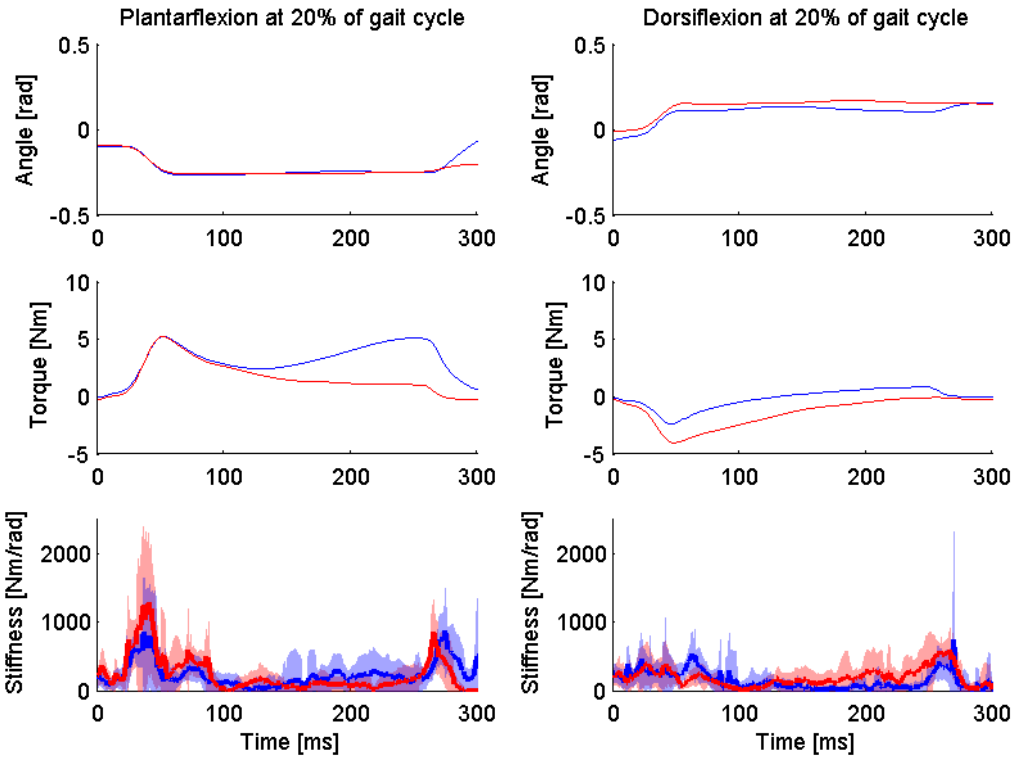

Figure 7.7: Summary of results from perturbations at 20% of gait cycle in plantarfelxion direction (*left*) and dorsiflexion (*right*). Blue lines show results from the dynamic experiment; red lines show isometric results. Top and middle graphs are angular position and torque data, averaged across repeated sweeps of individual subjects (n=20), and across all subjects (n=11). Bottom graph shows ankle joint stiffness averages from all subjects (n=11), with shaded areas showing ± 1 SD.

during the dynamic experiment, maximum mean stiffness was 392,4 ± 722,0 Nm/rad. During the hold-release time (t = 266ms), the isometric stiffness values were 605,3 ± 366,1 Nm/rad and 311,8 ± 318,9 Nm/rad for dynamic.

Summary:
The modulation of ankle stiffness investigated both during walking at a phase of 20% of gait cycle, and at the corresponding posture matching that phase is summarized on Table 7.2. The table shows the difference between mean stiffness values measured during the dynamic and isometric experiments ($K_{isometric} - K_{dynamic}$), and investigated at two timings: the initial phase when a perturbation is applied, and at the hold release moment (t = 41 ms and t = 274ms respectively, Fig. 7.7 on page 52). If the difference is positive, the mean stiffness measured during the isometric experiment is greater than during the dynamic.

Table 7.2 shows that mean stiffness values measured during isometric conditions are higher during the initial perturbation phase than during dynamic experiment at a phase of 20% of gait cycle for both plantarflexion and dorsiflexion measurements. At the end of the perturbation (hold release), mean stiffness values measured isometrically are in fact lower than during the dynamic experiment both plantarflexion and dorsiflexion perturbations.

Perturbation direction	$K_{isometric} - K_{dynamic}$	
	Initial phase	**Hold release**
Plantarflexion	575.2 [Nm/rad]	-17.7 [Nm/rad]
Dorsiflexion	12.6 [Nm/rad]	-142.3 [Nm/rad]

Table 7.2: Summary of the ankle stiffness modulation investigated both during walking at a phase of 20% of gait cycle (*dynamic*), and at the corresponding posture matching that phase *isometric*.

7.3.3 Dynamic and isometric comparison at 50% of the gait cycle

Figure 7.8 shows a comparison of the angular position and torque data, averaged across repeated sweeps of individual subjects (n=20), and across all subjects (n=11 for plantarflexion and n=10 subject for dorsiflexion), as well as modulation of the ankle joint stiffness during walking 50% of gait cycle in plantarflexion direction (*left*) and dorsiflexion (*right*). One subject had to be excluded from the analysis due to inconsistent measurements that had been related to equipment malfunction. Figure 7.8 also shows the period between the onset of perturbation (time 0s) and the end of the hold time (time 0.3s).

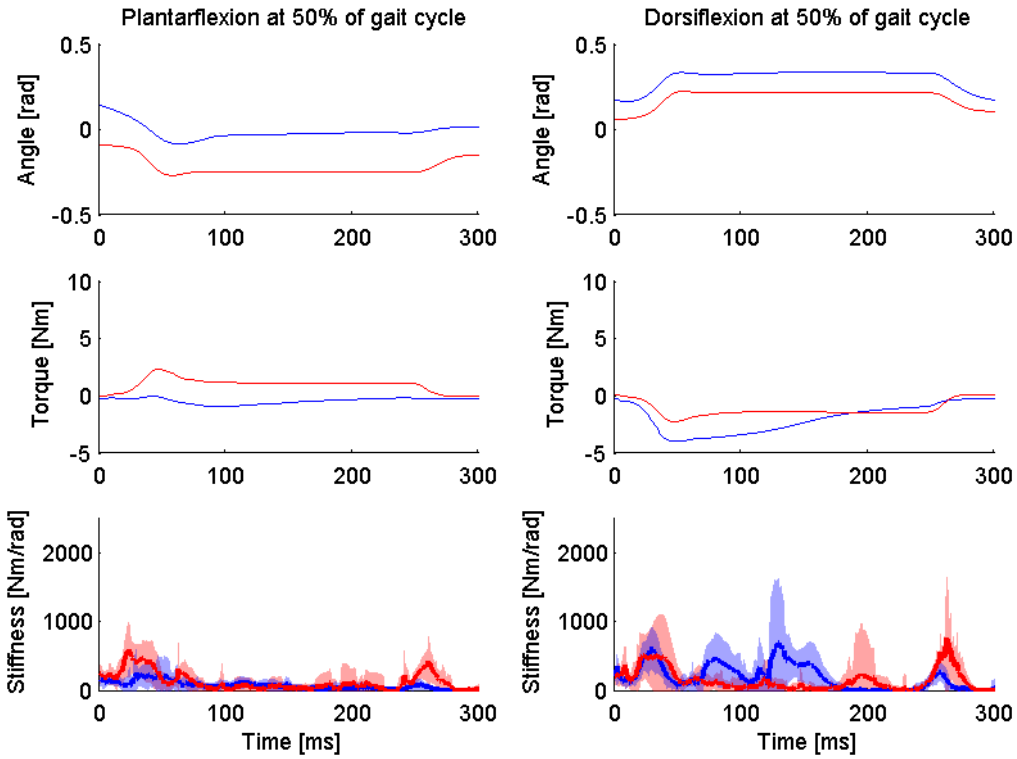

Figure 7.8: Summary of results from perturbations at 50% of gait cycle in plantarflexion direction (*left*) and dorsiflexion (*right*). Blue lines show results from the dynamic experiment; red lines show isometric. Top and middle graphs are angular position and torque data, averaged across repeated sweeps of individual subjects (n=20), and across all subjects (n=11 for plantarflexion and n=10 subject for dorsiflexion). Bottom graph shows ankle joint stiffness averages from all subjects (n=11 plantarflexion, n=10 dorsiflexion), with shaded areas showing ± 1 SD.

At the initial phase of the perturbation during *plantarflexion* (t = 25 ms) (Fig. 7.8, *left*), the maximum peak isometric stiffness was 598,9 ± 395,2 Nm/rad, whereas at the same timing during the dynamic trial, maximum mean stiffness was 265,2 ± 362,7 Nm/rad. During the hold-release time (t = 260ms), the isometric stiffness values were 431,7 ± 366,0 Nm/rad for isometric and 101,4 ± 82,7 Nm/rad for dynamic.

During *dorsiflexion* (7.8, *right*), at the initial phase of the perturbation (t = 30 ms) the maximum peak isometric stiffness was 491,3 ± 445,9 Nm/rad, and 617,6 ± 306,3 Nm/rad during the dynamic experiment. At the hold-release time (t = 260ms), the isometric stiffness peak values were 764,9 ± 889,0 Nm/rad for isometric and 286,5 ± 145,0 Nm/rad during dynamic.

Summary:
The modulation of ankle stiffness investigated both during walking at a phase of 50% of gait cycle, and at the corresponding posture matching that phase is summarized on Table 7.3. The table shows the difference between mean stiffness values measured during the dynamic and isometric experiments, and investigated at two timings: the perturbation initiation phase, and at the hold release time (t = 30 ms and t = 260 ms respectively, Fig. 7.8, page 53).

Perturbation direction	$\mathbf{K_{isometric} - K_{dynamic}}$	
	Initial phase	**Hold release**
Plantarflexion	333.7 [Nm/rad]	330.3 [Nm/rad]
Dorsiflexion	-126.3 [Nm/rad]	478.4 [Nm/rad]

Table 7.3: Summary of the ankle stiffness modulation investigated during walking at a phase of 50% of gait cycle (*dynamic*), and at the corresponding leg posture matching that phase *isometric*

Table 7.3 indicates that the mean stiffness values measured during isometric conditions are higher during the initial perturbation phase than during dynamic experiment at a phase of 50% of gait cycle for plantarflexion only (mean isometric stiffness 333.7 Nm/rad greater than dynamic). At dorsiflexion, however, the isometric stiffness was lower than dynamic. At the end of the perturbation (hold–release), mean stiffness values measured isometrically were lower than during the dynamic experiment for both plantarflexion and dorsiflexion perturbations.

7.3.4 Dynamic and isometric comparison at 90% of the gait cycle

Figure 7.9 illustrates a comparison of the angular position and the resulting torque, averaged across repeated sweeps of individual subjects (n=20), and across all subjects (n=11), as well as modulation of the ankle joint stiffness during walking at 90% of gait cycle in plantarflexion direction (*left*) and dorsiflexion (*right*).

At the initial phase of the perturbation during the *plantarflexion* measurement, (t = 25 ms) (Fig. 7.9, *left*), the maximum measured peak isometric stiffness was 656 ± 169,4 Nm/rad, whereas at the same timing during the dynamic trial, the maximum mean stiffness peak was 308,9 ± 245,1 Nm/rad. During the hold-release time (t = 258 ms), the isometric peak stiffness mean values were 473,6 ± 143,9 Nm/rad for isometric and 686,1 ± 451,2 Nm/rad for dynamic.

During *dorsiflexion* (7.9, *right*), at the initial phase of the perturbation (t = 24 ms) the maximum peak isometric stiffness was 745,2 ± 302,8 Nm/rad, and 162,8 ± 116,8 Nm/rad during the dynamic experiment. At the hold-release time (t = 255 ms), the isometric stiffness peak values were 616,5 ± 281,4 Nm/rad for isometric and 722 ± 275,2 Nm/rad during dynamic.

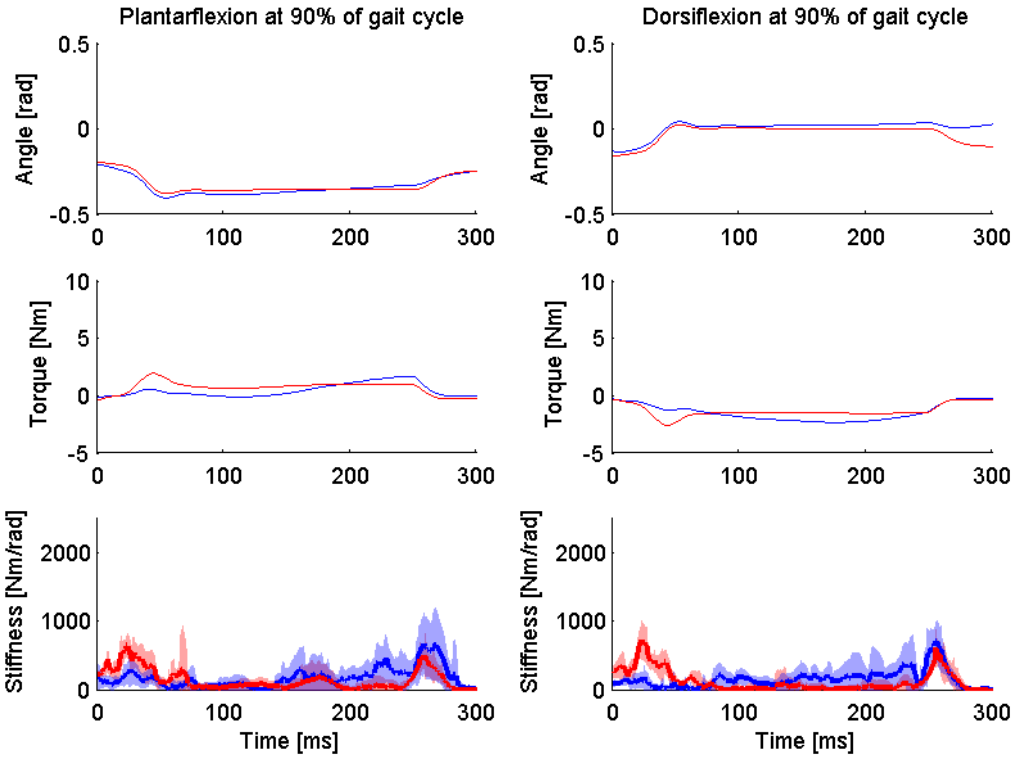

Figure 7.9: Perturbation results at 90% of gait cycle in plantarflexion (*left*) and dorsiflexion directions (*right*). Blue lines show results from the dynamic experiment; red lines show isometric results. Top and middle graphs are angular position and torque data, averaged across repeated sweeps of individual subjects (n=20), and across all subjects (n=11). Bottom graph shows ankle joint stiffness averages from all subjects (n=11), with shaded areas showing ± 1 SD.

Summary:
Ankle stiffness modulation investigated during walking at a phase of 90% of gait cycle, and at the corresponding posture matching that phase, is abridged on Table 7.4. The table illustrates the difference between mean stiffness values measured during dynamically and isometrically,

and investigated at two timings: the perturbation initiation phase, and at the hold release time (t = 25 ms and t = 256 ms respectively, Fig. 7.9, page 55).

Perturbation direction	$\mathbf{K_{isometric} - K_{dynamic}}$ **Initial phase**	**Hold release**
Plantarflexion	347.1 [Nm/rad]	-212.5 [Nm/rad]
Dorsiflexion	582.4 [Nm/rad]	-105.5 [Nm/rad]

Table 7.4: Summary of the ankle stiffness modulation investigated both during walking at a phase of 90% of gait cycle (*dynamic*), and at the corresponding leg posture matching that phase *isometric*

Table 7.4 demonstrates that the mean stiffness values measured during isometric conditions are also higher during the initial perturbation phase than during dynamic experiment at a phase of 90% of gait cycle for for both plantarflexion and dorsiflexion measurements. At the end of the perturbation (hold–release), mean stiffness values measured isometrically were lower than during the dynamic experiment for both plantarflexion and dorsiflexion perturbations.

7.3.5 Stiffness modulation between phases

Figure 7.10 shows the comparison between averaged (n=11) stiffness values for perturbations during different phases of gait, for both the dynamic (**A** and **B**, *left* on Fig. 7.10) and the isometric (**C**, and **D**, *right* on Fig. 7.10) trials. Stiffness estimates are plotted over a 300 ms window, starting at perturbation onset (t=0 ms) until after the end of the hold phase (t=300 ms).

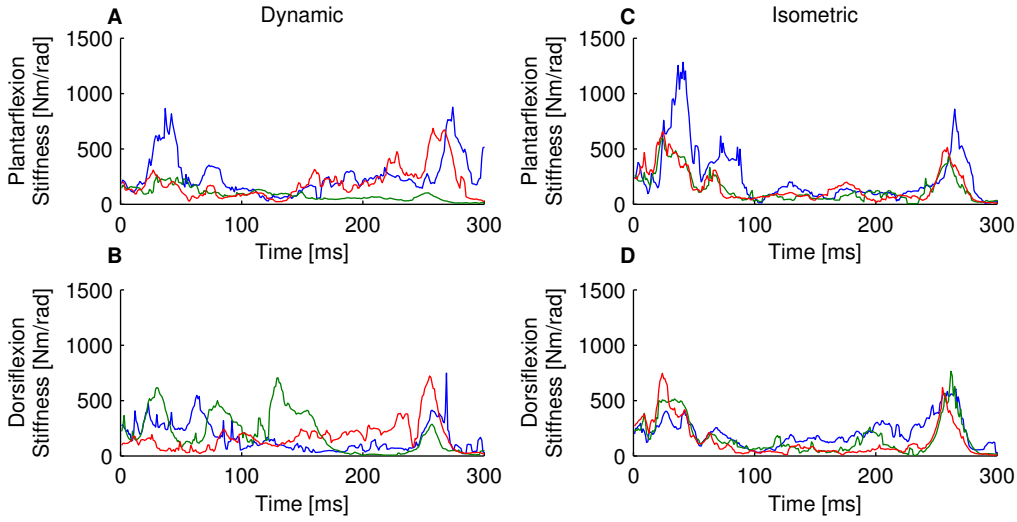

Figure 7.10: Summary of the ankle stiffness modulation investigated between phases of gait cycle during dynamic experiment (**A** and **B**, *left*), and isometric (**C** and **D**, *right*). Blue lines correspond to stiffness at 20% of gait cycle, green lines correspond to 50%, and red lines to 90%.

It can be seen on Figure 7.10 that the highest stiffness values were estimated for the plantarflexion perturbations during 20% of gait cycle, both dynamic and isometric (blue lines on **A** and **C**, in Fig. 7.10). The peak stiffness value in isometric plantarflexion trials was found at the initial perturbation phase (between approximately 0 ms and 50 ms), for 20% isometric plantarflex-

ion, and was estimated to be 1283 ± 1029 Nm/rad. This was 627 Nm/rad higher than the next highest value of 656.0 ± 169.4 Nm/rad, at 90% isometric plantarflexion.

At the dynamic plantarflexion trials, the peak stiffness value was found after the end of the hold phase (between approximately 250 ms and 300 ms), for the 20% perturbation trial, and was 877.0 ± 677.6 Nm/rad. This was 190.9 Nm/rad higher, than the next highest value of 686.1 ± 451.2 Nm/rad, at 90% dynamic plantarflexion.

For the dorsiflexion trials (**B** and **D**, in 7.10), more profound differences could be seen between the dynamic and isometric trials. The stiffness values for isometric trials exhibited a similar behavior throughout the 20%, 50%, and 90% perturbation trials, with distinct peaks at the initial phase, after the hold phase, and during a low plateau between them. Peak values during the initial phase were 405.0 ± 336.9 Nm/rad, 491.3 ± 445.9 Nm/rad, and 745.2 ± 302.8 Nm/rad for the 20%, 50%, and 90% trials respectively. Peak values after the hold phase were 605.3 ± 366.1 Nm/rad , 764.9 ± 889.0 Nm/rad, and 616.5 ± 281.4 Nm/rad for the 20%, 50%, and 90% trials respectively.

However, the stiffness estimates for the dynamic dorsiflexion trials showed a behavior not exhibited in any other combination. At the initial phase of perturbation, no clear, common peak can be observed. After the end of the hold phase, the peak stiffness value was 722.0 ± 275.2 Nm/rad, for the 90% perturbation. The peak value for the dynamic dorsiflexion at 50% perturbation was found to be 705.0 ± 925.9 Nm/rad, at t = 130 ms, which was during the perturbation hold phase.

Part III

Synthesis

CHAPTER 8

DISCUSSION

Experimental measurements of ankle stiffness during dynamic conditions similar to those of unimpaired locomotion are of a great importance if one understanding how posture, gait and the mechanical properties of our limbs are regulated by the central nervous system. The mechanical properties of our joints provide the means to interact with the physical world, and our understanding of they are regulated during unimpaired locomotion is therefore crucial.

A common approach for estimating ankle joint stiffness consists of perturbing the joint in a controlled manner during isometric experiments, where subjects usually lie supine or sit with their foot attached to a servo–motor by fiber–glass cast boots. Such an experiment design is a result of the necessity to have the subject's limb attached rigidly when perturbations are applied to the joint, which is associated with considerable experimental challenges, but also prohibits the use of such design in walking studies. As a result, one uses model predictions attempt to predict joint stiffness for angular position and different levels of torque, as it is difficult to investigate in experimental conditions [Zajac et al. 1989, Cui et al. 2008, Pfeifer et al. 2012] Consequently, ankle joint stiffness has mostly been investigated during static conditions. However, in order to properly understand the modulation of such stiffness during unimpaired gait, there is a need for dynamic experiments.

The use of the mobile ankle and knee perturbator in this study allowed maintaining an unimpaired gait for the subjects while providing accurate perturbations to the ankle joint without impeding natural gait at the same time.

Experimental considerations

The use of a metronome in the experiment design in order to help the subjects maintain the rhythm of walking with constant speed was an effective solution. It was crucial that subjects maintained a constant stride duration. That ensured that the recordings were only made for comparable steps, and the perturbations were applied at the correct time of the gait cycle. The gait cycle length was being monitored on–line during the dynamic part of the experiment. The recorded average gait cycle durations across all subjects differed moderately in between the

subjects, which was a result of each subject choosing their own comfortable walking speed. The standard deviation values of the mean gait cycle duration for every subject were very low. Consequently, there was no significant variation of the gait cycle durations between the subjects, which secured the correct perturbation-application timings throughout the dynamic part of the experiment.

During data collection, a number of recordings showed evidence of malfunctioning strain gauge readings. Based on the intermittent nature of the problem and features of the signal anomalies, i.e. momentary offset jumps, sometimes causing signal saturation, a loose signal connection to the strain gauge was diagnosed. Whenever the torque data showed evidence of strain gauge malfunction it was removed from the data pool, and if the data corruption was noticed during the data recording session, additional sweeps were recorded to replace the deleted ones. However, some corrupted sweeps were not noticed during the on–line validation and were included in the collected data pool. These sweeps were then removed as part of data processing, causing the data population to shrink. This was not a problem apart from in the case of Subject 9, where dynamic data from dorsiflexion perturbations at 50% of gait cycle were too corrupted to be included in the analysis.

It was an important consideration to ensure the quality of the coupling between the functional joint and the subject's legs. The first consideration was that the carbon–fiber cast sat comfortably, so that its presence would not alter the subject's gait and that long lasting experiments could be carried out. Lack of physical discomfort was a contributing factor in the subjects' keeping a steady walking profile throughout the experiments. Secondly, and at least equally importantly, the quality of the coupling was crucial in properly transferring the perturbation from the actuator to the ankle joint. The coupling needed to be rigid enough to transfer the torque from the motor to the ankle joint system.

Discussion of results

It was the hypothesis of this project that the stiffness of the human ankle joint measured during dynamic conditions was lower than stiffness measured isometrically. To that end, an experimental design was used, which allowed the estimation of stiffness during dynamic conditions of walking and then during isometric conditions, where the static poses used were closest approximations possible of the corresponding conditions during walking.

Results described in Chapter 7, showed that there is a non–significant difference between the mean values of joint stiffness during dynamic and isometric trials (P = 0.77383). Upon further inspection of the results (shown in figures 7.7, 7.8, 7.9 and summarized in Figure 7.10, page 56) the calculated stiffness values were found to have higher magnitudes for the isometric trials than those of the dynamic trials. This was most profound during the initial perturbation phase (approximately between 0 ms and 80 ms) where the perturbation elicits the highest change in position and provokes a high torque variation.

Additionally, a statistically significant difference in mean ankle stiffness was found between the three phases of gait cycle during the plantarflexion measurements only [$P < 0.0005$]. This is considered to be caused by the fact, that joint stiffness is modulated throughout the gait cycle. Since the three gait phases, at which perturbations were applied, are characterised by different conditions, such as joint angle, body weight support and contact with the ground, it

was expected to find evidence of stiffness modulation between these conditions.

However, it was observed that large standard deviation values were present in some of the stiffness estimates. Indeed, as the example in Figure 8.1 shows, the model was not robust enough, and provided stiffness estimates that varied also within individual subjects, leading to large standard deviations of the averages.

This was also magnified by the fact that stiffness IRFs can be difficult to inspect visually and can change rapidly between realizations. It is speculated, that the large standard deviations in the models estimates could partially be reduced if the data population was increased. This could be achieved by enlisting more subjects, or recording more repetitions of perturbations in each combination of direction and gait cycle phase. However, more perturbation repetitions would impose a considerably longer experiment duration, which could be challenging.

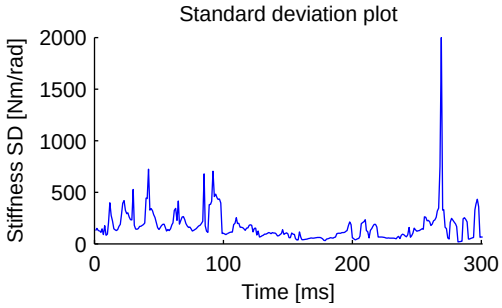

Figure 8.1: Example of the standard deviation of a stiffness estimate. Graph shows SD for results from dynamic dorsiflexion perturbation at 20% of gait cycle.

Contextualisation of results

In order to obtain joint stiffness estimations, one studies joint impedance, since is important to remember that joint stiffness is only one component of joint impedance. Inertial, viscous, and other properties also contribute substantially to the mechanical properties of a limb.

Literature suggests that joint impedance is believed to be lower dynamic movement conditions when compared to static conditions. One potential explanation is that the neural control of movement is substantially different than that of posture Ludvig et al. [2012]. Studies by Latash & Gottlieb [1991] and Bennett et al. [1992] have shown that joint impedance is lower during movement than during maintenance of a fixed posture in human elbow joint. Ludvig et al. [2012] demonstrated that knee impedance during dynamic conditions is much lower than would be predicted from isometric studies. Our results show a similar tendency for stiffness to be lower during dynamic experiments, where during perturbation-initalization, the maximum mean stiffness was lower in dynamic trials than in isometric for phases 20% and 90%, both plantar– and dorsiflexion, and in 50% for plantarflexion.

The study by Mirbagheri et al. [2000] analysed the intrinsic mean stiffness of the ankle joint in isometric conditions, where subjects lay supine with their foot attached to an actuator. The study found stiffness to range between the lowest value of 224 Nm/rad to the highest at 377 Nm/rad (with mean 325 Nm/rad and SD 72 Nm/rad) in trials involving pseudo-random binary sequence position perturbations (PRBS). When subjects were instructed to maintain a constant level of torque in a separate procedure, intrinsic stiffness reached the lowest value of 310 Nm/rad to the highest at 509 Nm/rad (with mean 412 Nm/rad and SD 64 Nm/rad).

Studies investigating ankle stiffness in dynamic conditions usually implement force platforms, and while they involve different conditions than the ones investigated in our study, such find-

ings help contextualise our results.Stefanyshyn & Nigg [1998] reported ankle joint stiffness values of 5.68 Nm/deg in running 7.38 Nm/deg in sprinting respectively (325 Nm/rad in running and 422.8, sprinting) in experiments involving stiffness estimations by means of force platforms. The study by Kuitunen et al. [2002] showed that ankle joint stiffness and increased from 974 to 1375 Nm/rad with increasing running speed. Mean stiffness estimates in our study were therefore within the order of magnitude comparable to results found in literature.

BIBLIOGRAPHY

M. Abe & N. Yamada (2003). 'Modulation of elbow joint stiffness in a vertical plane during cyclic movement at lower or higher frequencies than natural frequency'. Experimental brain research **1**53(3):394–399.

G. Agarwal & C. Gottlieb (1977). 'Compliance of the human ankle joint'. Journal of Biomechanical Engineering **9**9:166.

J. B. Andersen & T. Sinkjaer (1995). 'An actuator system for investigating electrophysiological and biomechanical features around the human ankle joint during gait'. Rehabilitation Engineering, IEEE Transactions on **3**(4):299–306.

J. B. Andersen & T. Sinkjær (2003). 'Mobile ankle and knee perturbator'. Biomedical Engineering, IEEE Transactions on **5**0(10):1208–1211.

R. S. Behnke (2006). Kinetic Anatomy. Human Kinetics.

D. Bennett, et al. (1992). 'Time-varying stiffness of human elbow joint during cyclic voluntary movement'. Experimental Brain Research **8**8(2):433–442.

F. Bojsen-Møller (2009). Bevægeapparatets anatomi. Munksgaard Danmark.

C. Capaday (2002). 'The special nature of human walking and its neural control'. Trends in neurosciences **2**5(7):370–376.

R. Crowninshield, et al. (1976). 'An analytical model of the knee'. Journal of Biomechanics **9**(6):397–405.

L. Cui, et al. (2008). 'Modeling short-range stiffness of feline lower hindlimb muscles'. Journal of biomechanics **4**1(9):1945–1952.

R. A. Donatelli (1996). The Biomechanics of the Foot and Ankle. F. A. Davis Company.

C. T. Farley, et al. (1998). 'Mechanism of leg stiffness adjustment for hopping on surfaces of different stiffnesses'. Journal of Applied Physiology **8**5(3):1044–1055.

D. P. Ferris & C. T. Farley (1997). 'Interaction of leg stiffness and surface stiffness during human hopping'. Journal of applied physiology **8**2(1):15–22.

D. P. Ferris, et al. (1998). 'Running in the real world: adjusting leg stiffness for different surfaces'. Proceedings of the Royal Society of London. Series B: Biological Sciences **2**65(1400):989–994.

P. Gatev, et al. (2004). 'Feedforward ankle strategy of balance during quiet stance in adults'. The Journal of physiology **5**14(3):915–928.

A. H. Hansen, et al. (2004). 'The human ankle during walking: implications for design of biomimetic ankle prostheses'. Journal of biomechanics **3**7(10):1467–1474.

X. Hu, et al. (2011). 'Muscle short-range stiffness can be used to estimate the endpoint stiffness of the human arm'. Journal of Neurophysiology **1**05(4):1633–1641.

I. Hunter & R. Kearney (1982). 'Dynamics of human ankle stiffness: variation with mean ankle torque'. Journal of Biomechanics **1**5(10):747–752.

S. Kapp, et al. (2009). 'Lower limb prosthetics'. Pasquina PF, Cooper RA. Care of the combat amputee. Washington, DC: Borden Institute pp. 553–80.

R. Kearney & I. Hunter (1982). 'Dynamics of human ankle stiffness: variation with displacement amplitude'. Journal of biomechanics **1**5(10):753–756.

R. E. Kearney, et al. (1990). 'System identification of human joint dynamics.'. Critical reviews in biomedical engineering **1**8(1):55.

R. E. Kearney, et al. (1997). 'Identification of intrinsic and reflex contributions to human ankle stiffness dynamics'. Biomedical Engineering, IEEE Transactions on **4**4(6):493–504.

R. F. Kirsch, et al. (1992). 'Performance of ensemble time-varying system identification methods: Analog simulations and biological applications'. In Engineering in Medicine and Biology Society, 1992 14th Annual International Conference of the IEEE, vol. 6, pp. 2754–2755. IEEE.

S. Kuitunen, et al. (2002). 'Knee and ankle joint stiffness in sprint running'. Medicine and science in sports and exercise **3**4(1):166–173.

S. Lark, et al. (2003). 'Adequate joint stiffness is critical during the single support phase to control forward and downward body momentum'. Clin Biomech **1**8:848–855.

M. Latash & G. Gottlieb (1991). 'Reconstruction of shifting elbow joint compliant characteristics during fast and slow movements'. Neuroscience **4**3(2):697–712.

I. D. Loram & M. Lakie (2002). 'Direct measurement of human ankle stiffness during quiet standing: the intrinsic mechanical stiffness is insufficient for stability'. The journal of physiology **5**45(3):1041–1053.

D. Ludvig, et al. (2007). 'Voluntary modulation of human stretch reflexes'. Experimental Brain Research **1**83(2):201–213.

D. Ludvig & R. Kearney (2007). 'Real-time estimation of intrinsic and reflex stiffness'. Biomedical Engineering, IEEE Transactions on **5**4(10):1875–1884.

D. Ludvig & E. Perreault (2011a). 'Estimation of joint impedance using short data segments'. In Engineering in Medicine and Biology Society, EMBC, 2011 Annual International Conference of the IEEE, pp. 4120–4123. IEEE.

D. Ludvig & E. Perreault (2011b). 'System Identification of Physiological Systems Using Short Data Segments' .

D. Ludvig, et al. (2012). 'Time-Varying System Identification for Understanding the Control of Human Knee Impedance'. In System Identification, vol. 16, pp. 1306–1310.

F. H. Martini & J. L. Nath (2009). Fundamentals of anatomy and physiology. Pearson.

M. Mirbagheri, et al. (2000). 'Intrinsic and reflex contributions to human ankle stiffness: variation with activation level and position'. Experimental brain research **1**35(4):423–436.

M. Nordin & V. H. Frankel (2012). Ankle Biomechanics of the Musculoskeletal System. Lippincott Williams & Wilkins.

S. Pfeifer, et al. (2012). 'Model-Based Estimation of Knee Stiffness'. Biomedical Engineering, IEEE Transactions on **5**9(9):2604–2612.

F. Popescu, et al. (2003). 'Elbow impedance during goal-directed movements'. Experimental brain research **1**52(1):17–28.

A. Roy, et al. (2011). 'Measurement of passive ankle stiffness in subjects with chronic hemiparesis using a novel ankle robot'. Journal of Neurophysiology **1**05(5):2132–2149.

T. Sinkjaer, et al. (2004). 'Major role for sensory feedback in soleus EMG activity in the stance phase of walking in man'. The Journal of physiology **5**23(3):817–827.

T. Sinkjær, et al. (1996). 'Soleus stretch reflex modulation during gait in humans'. Journal of Neurophysiology **7**6(2):1112–1120.

T. Sinkjaer, et al. (1988). 'Muscle stiffness in human ankle dorsiflexors: intrinsic and reflex components'. Journal of Neurophysiology **6**0(3):1110–1121.

D. J. Stefanyshyn & B. Nigg (1998). 'Dynamic angular stiffness of the ankle joint during running and sprinting'. Journal of applied biomechanics **1**4:292–299.

R. Stein & R. Kearney (1995). 'Nonlinear behavior of muscle reflexes at the human ankle joint'. Journal of neurophysiology **7**3(1):65–72.

C. Tai & C. Robinson (1999). 'Knee elasticity influenced by joint angle and perturbation intensity'. Rehabilitation Engineering, IEEE Transactions on **7**(1):111–115.

R. Trumbower, et al. (2009). 'Use of self-selected postures to regulate multi-joint stiffness during unconstrained tasks'. PloS one **4**(5):e5411.

P. Weiss, et al. (1988). 'Human ankle joint stiffness over the full range of muscle activation levels'. Journal of biomechanics **2**1(7):539–544.

P. Weiss, et al. (1986). 'Position dependence of stretch reflex dynamics at the human ankle'. Experimental brain research **6**3(1):49–59.

D. T. Westwick & E. J. Perreault (2006). 'Identification of apparently acausal stiffness models'. In Engineering in Medicine and Biology Society, 2005. IEEE-EMBS 2005. 27th Annual International Conference of the, pp. 5611–5614. IEEE.

F. E. Zajac et al. (1989). 'Muscle and tendon: properties, models, scaling, and application to biomechanics and motor control.'. Critical reviews in biomedical engineering **1**7(4):359.

J. Zar (2010). Biostatistical analysis. Pearson Education International, 5 edn.

L. Zhang, et al. (1997). 'In vivo human knee joint dynamic properties as functions of muscle contraction and joint position'. Journal of biomechanics **3**1(1):71–76.

Zygote Media Group (2013). 'Zygote Body'. www.zygotebody.com.

Part IV

Appendix

APPENDIX A

STATISTICAL ANALYSIS

A.1 Walking profiles across the subjects

The average gait cycle duration was calculated for each individual subject five times during the dynamic part of the experiment. These durations for each subject are shown on Table A.1. The first measurement (Duration 1.) was made at the beginning of the experiment, during the walking profile measurement. Measurements numbered 2,3,4 and 5 were taken later in the dynamic experiment. In some subjects, the isometric experiment was carried out first, and therefore there was an approximately 30 minutes pause between the first measurement and the other four.

Gait cycle durations during experiment

Subject no.	Duration 1.	Duration 2.	Duration 3.	Duration 4.	Duration 5.	Mean [s]	SD [s]
1	1.150	1.130	1.150	1.150	1.155	1.150	0.010
2	1.090	1.080	1.120	1.095	1.095	1.096	0.015
3	1.230	1.205	1.210	1.220	1.215	1.216	0.010
4	1.065	1.095	1.080	1.060	1.090	1.078	0.015
5	1.140	1.130	1.190	1.145	1.130	1.147	0.025
6	1.069	1.120	1.078	1.090	1.125	1.096	0.025
7	1.095	1.080	1.095	1.095	1.080	1.089	0.008
8	1.120	1.120	1.120	1.130	1.110	1.120	0.007
9	1.315	1.275	1.270	1.270	1.280	1.282	0.019
10	1.250	1.140	1.140	1.130	1.120	1.156	0.053
11	1.250	1.245	1.260	1.260	1.245	1.252	0.008

Table A.1: Gait cycle durations of the 11 subjects during the dynamic part of the experiment.

The mean value of the gait cycle duration for all the 11 subjects was 1.160 second [SD=0.070

second].

A.2 Two-Factor Analysis of Variance

The data obtained in both the dynamic and isometric experiments require a two-way analysis of variance. The two examined factors are fixed and consist of:

- Factor A: dynamic or isometric measurement
- Factor B: phases of gait cycle

The variable under consideration is the mean value of ankle joint stiffness.

The means of all the sets within Factor A (dynamic or isometric measurement) and Factor B (phases of gait cycle) were analyzed with a two-factor ANOVA. ANOVA, which stands for *analysis of variance*, is a collection of statistical procedures, in which the observed variance in a particular variable is partitioned into components attributable to different sources of variation [Zar 2010].

Specifically, a two-factor ANOVA tests the following hypotheses:

- H_0: There is no effect of the type of experiment, dynamic or isometric, on the mean ankle stiffness during perturbation ($\mu_{dynamic} = \mu_{isometric}$)
- H_A: There is an effect of the type of experiment, dynamic or isometric, on the mean ankle stiffness during perturbation ($\mu_{dynamic} \neq \mu_{isometric}$)
- H_0: There is no difference in mean ankle stiffness between the three phases of gait cycle ($\mu_{20\%} = \mu_{50\%} = \mu_{90\%}$)
- H_A: There is a difference in mean ankle stiffness between the three phases of gait cycle ($\mu_{20\%}, \mu_{50\%}, \mu_{90\%}$ are not the same.)
- H_0: There is no interaction between the type of experiment (dynamic or isometric) and the phase of gait cycle on the mean ankle stiffness.
- H_A: There is an interaction between the type of experiment (dynamic or isometric) and the phase of gait cycle on the mean ankle stiffness.

where μ is a mean of the ankle stiffness.

The critical value for this test is $F_{\alpha(1),(k-1),(N-k)}$, which is the value of F at the one-tailed significance level of α, where k is the number of groups and N is the total number of samples. If the calculated value of F is as large as the critical value of F, or large than that, then the null hypothesis must be rejected [Zar 2010].

A.2.1 Plantarflexion

An interaction between two factors means that the effect of one factors under investigation is not independent of the other factor. The following ANOVA has been carried out to investigate the two factors in plantarflexion measurements:

2×3 two-factor ANOVA results			
Source of variation	SS	DF	MS
Total	515610	65	
Factor A	387.88	1	387.88
Factor B	211793.83	2	105896.92
A × B	20828.43	2	10414.22
Within Cells Error	10414.22	60	4710

Table A.2: Two-factor ANOVA results for the plantarflexion experiments.

F and P values		
.:	F	P
Factor A	0.08	0.7783
Factor B	22.48	<0.0001
A × B	2.21	0.1186

Table A.3: F and P values for the two-factor ANOVA for plantarflexion experiments.

For H_0: There is no effect of the type of experiment, dynamic or isometric, on the mean ankle stiffness during perturbation ($\mu_{dynamic} = \mu_{isometric}$):

$$F = \frac{FactorAMS}{ErrorMS} = \frac{387.88}{4710} = 0.08 \tag{A.1}$$

The critical value for F is:

$$F_{\alpha(1),(k-1),(N-k)} = F_{0.05(1),(2),(64)} = 2.74 \tag{A.2}$$

Therefore, do not reject H_0.

$P > 0.25$ [P = 0.77383] Thus, it can be concluded that the null hypothesis is true: there is no effect of the type of experiment, dynamic or isometric, on the mean ankle stiffness during perturbation ($\mu_{dynamic} = \mu_{isometric}$).

For H_0: There is no difference in mean ankle stiffness between the three phases of gait cycle ($\mu_{20\%} = \mu_{50\%} = \mu_{90\%}$):

$$F = \frac{FactorBMS}{ErrorMS} = 22.48 \tag{A.3}$$

The critical value for F is:

$$F_{0.05(1),(2),(64)} = 2.74 \tag{A.4}$$

Therefore, reject H_0.
$P < 0.0005$

Thus, it can be concluded with a 95% confidence that the average values of the ankle stiffness are not the same between the three different phases of the gait cycle.

For H_0: There is no interaction between the type of experiment (dynamic or isometric) and the phase of gait cycle on the mean ankle stiffness:

$$F = \frac{A \times BMS}{ErrorMS} = 2.21 \tag{A.5}$$

The critical value for F is:

$$F_{0.05(1),(2),(64)} = 2.74 \tag{A.6}$$

Therefore, do not reject H_0.
$0.05 < P < 0.10$ [P = 0.1186]

There is no interaction between the type of experiment (dynamic or isometric) and the phase of gait cycle on the mean ankle stiffness (i.e. accross the two factors).

A.2.2 Dorsiflexion

The following ANOVA has been carried out to investigate the two factors in dorsiflexion measurements:

Two-Factor ANOVA results

Source of variation	SS	DF	MS
Total	263329.22	64	
Factor A	239.79	1	239.79
Factor B	10733.34	2	5366.67
A × B	21365.48	2	10682.74
Within Cells Error	230990.61	59	3915.1

Table A.4: Two-factor ANOVA results for the dorsiflexion experiments.

F and P values

.:	F	P
Factor A	0.06	0.8073
Factor B	1.37	0.2621
A × B	2.73	0.0735

Table A.5: F and P values for the two-factor ANOVA for dorsiflexion experiments.

For H_0: There is no effect of the type of experiment, dynamic or isometric, on the mean ankle stiffness during perturbation ($\mu_{dynamic} = \mu_{isometric}$):

$$F = \frac{FactorAMS}{ErrorMS} = 0.06 \tag{A.7}$$

The critical value for F is:

$$F_{\alpha(1),(k-1),(N-k)} = F_{0.05(1),(2),(64)} = 2.74 \tag{A.8}$$

Therefore, do not reject H_0. $0.05 < P < 0.10$ [P = 0.8073]

For H_0: There is no difference in mean ankle stiffness between the three phases of gait cycle ($\mu_{20\%} = \mu_{50\%} = \mu_{90\%}$):

$$F = \frac{FactorBMS}{ErrorMS} = 1.37 \tag{A.9}$$

The critical value for F is:

$$F_{0.05(1),(2),(64)} = 2.74 \tag{A.10}$$

Therefore, do not reject H_0. $P > 0.25$ [P = 0.2621]

For H_0: There is no interaction between the type of experiment (dynamic or isometric) and the phase of gait cycle on the mean ankle stiffness:

$$F = \frac{A \times BMS}{ErrorMS} = 2.73 \tag{A.11}$$

The critical value for F is:

$$F_{0.05(1),(2),(64)} = 2.74 \tag{A.12}$$

Therefore, do not reject H_0. $0.05 < P < 0.10$ [P = 0.0735]

A.3 Tukey HSD for *Post-Hoc* Analysis

If the ANOVA test shows that the means are in fact not all equal, the next step is to determine which means are different. The rejection of the null hypothesis does not mean that all the means are different from each other, and it is important to analyse how many differences there are, and precisely where the differences are between the means. In such case, it would be unreliable to employ multiple two-sample t-tests to examine the difference between more than two means, since this would greatly increase the likelihood of obtaining a Type I error. Instead, a multiple-comparison procedure needs to be performed.

For a total of *k* number of means, there are *k(k-1)/2* different ways to obtain pairs of means. For Factor B, there are k=3 means (corresponding to 20%, 50%, 90% of gait cycle duration).

Two-factor ANOVA statistical analysis for the plantarflexion experiments rejected the following null hypothesis:

- H_0: There is no difference in mean ankle stiffness between the three phases of gait cycle ($\mu_{20\%} = \mu_{50\%} = \mu_{90\%}$)

with the p value of $P < 0.0005$. The post-hoc analysis should only be performed if the ANOVA test shows a p-value less than the value of α. If $p > \alpha$, it is unknown whether or not the means

are all the same. Therefore, this analysis is only performed to investigate the null hypothesis above.

The *Tukey honestly significant difference (HSD)* test is almost analogous to a *t* score for each pair of means, but it is not compared to the Student's t distribution. Instead, a different distribution is used, called the studentized range (or *q* distribution), where q is the relevant critical value of the studentized range statistic.

If sample sizes are equal, the risk of a Type I error is α, and if sample sizes are unequal, it is less than α.

The three groups tested by the Tukey test are the 20%, 50%, 90% phases, both from the dynamic and isometric experiment. The summary of this *post-hoc* analysis is shown on Table A.6 and the results are shown on Table A.7:

Summary of the group means.

Group	Sample Mean	Sample size
20%	252.4364	22
50%	114.0659	22
90%	174.2677	22

Table A.6: Summary of the means of the three groups (20%, 50%, 90% phases), (sample size n=22 for each group).

For the purpose of this analysis, the mean values of ankle stiffness during the three phases of the gait cycle, 20%, 50%, 90% were analysed for *both* dynamic and isometric experiment, resulting in 22 samples per group. This part of the Tukey test evaluates the means only within Factor B (phases of gait cycle), and since the ANOVA analysis showed no significant difference between mean values of the dynamic and isometric experiment, the Tukey test included the stiffness mean values from both dynamic and isometric experiments (resulting in $n = 2 \times 11$ samples = 22 samples per group).

The Tukey test was performed for the critical value of $q_{\alpha,\nu,k} = q_{0.05,60,3} = 3.40$ and the following results were obtained:

Tukey HSD *Post-Hoc* analysis results.

Comparison	Absolute difference	Std. error of difference	Critical q	Conclusion
20%νs.50%	138.37	14.632	9.46	Means not equal
20%νs.90%	78.17	14.632	5.34	Means not equal
50%νs.90%	60.20	14.632	4.11	Means not equal

Table A.7: Tukey HSD *Post-Hoc* analysis results for the critical value of q=3.40.

Thus, it can be concluded that the mean stiffness value during the 20% phase is significantly different from 50%, and 90%, i.e. all means are different from each other ($\mu_{20\%} \neq \mu_{50\%} \neq \mu_{90\%}$).

APPENDIX B

INFORMED CONSENT

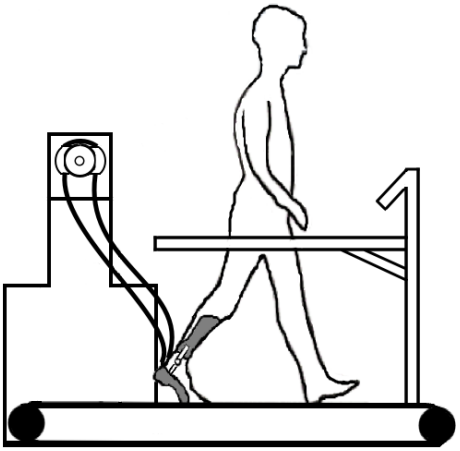

The purpose of this form is to give a clear explanation of the nature of this experiment. All the procedures involved are described below. If you at any time have questions or concerns after reading this form, please feel free to discuss these with the group members, and/or the supervisors of this project. Once you are entirely satisfied with this explanation and freely choose to participate in the study, you may indicate your inclination to participate by signing below. Remember that you are allowed to end your participation in the experiment at any time.

Purpose of the experiment

The purpose of the experiment is to investigate the ankle joint stiffness during walking and standing. The study of mechanical properties of human joints allows us to understand the complexities of interactions with the physical world and how these interactions are regulated. This study focuses on the human ankle and the dynamic relationship between perturbations of the ankle joint and the torque generated in response.

Procedure

The expected duration of the experiment is two hours. The experiment starts with preparation

of the subject's left leg, where the skin will be shaved and electrodes are attached to the skin. Casing will be placed on the lower left leg and attached firmly.

The experiment will be divided into two sessions: the walking part and standing part. During the walking session, you will be asked to walk on the treadmill with a comfortable walking speed, and perturbations will be applied to the ankle. Completion of this session will take approximately 25 minutes.

During the standing part, you will be asked to place your legs in three separate poses on the treadmill, and the same perturbations to the ankle will be applied during standing. Completion of this session will take approximately 30 minutes.
During both of the sessions, the activity of two of your muscles (EMG), as well as information of the position of your joint will be collected.

Risks and Discomfort
There is no risk of physical injury from participation in this study. There may be some discomfort from wearing the cast for a prolonged time. However, if you decide that you do not wish to participate in the study after it has started, please feel free to tell the researchers. There is no penalty if you decide to end your participation early.

All of the data recorded in the experiment are completely confidential. You will not be identified by name during the analysis of the data, only by a special number code. The results of your sessions will be combined with those of other participants and they will be studied only in this fashion. When the experiment results are presented, the data obtained from the experiment will also be reffered to with a number, and you will not be identified by name either.

You will not receive payment for your participation in this study, as it is strictly voluntary.

I understand that the procedures involved in this study involve minimal risks. Having acknowledged that, and after familiarising myself with the description of the project, I voluntarily agree to take part in the study. I have read this consent form and I understand all the procedures described in it. The researchers have explained to me anything I did not understand. Therefore, I agree to participate in this study.

_____ _____

Signature Date

_____

Researcher

APPENDIX C

EXPERIMENT PROTOCOL STEPWISE

Subject preparation

1. Let the subject try on a cast for fit. Fasten with velcro and have subject walk 5-10 strides on the treadmill to assess comfort. If cast needs changing, fit the next one and repeat the 5-10 strides. When the fit is comfortable, record video of the 5-10 strides.

2. Divide the workflow:

3. Cut out a recording of a single stride from the video. Run the matlab function to analyse the stride video.

4. Palpate TA and SOL muscles for optimal electrode placement. Shave and rinse electrode sites. Attach electrodes and leads. Ask subject to flex toes up, then stand on toes, each time checking signal on Mr. Kick.

5. Extract and note the distances and positions for both feet during the three phases.

6. Put on perturbator, fit the foam padding, put the tape around the cast and put the heel trigger on.

Measuring the gait pattern

1. Open an old WalkingProfile.mat file in MrKick, and then make a new file with the settings loaded
2. Start the treadmill and set 3.0 km/h
3. Let the subject find the preferred speed (if in doubt, suggest 3.9 km/h)
4. Once the subject is walking comfortably, start acquiring the 30 strides
5. Read of the mean stride duration from the 30 strides measurement and run through the matlab script to get the randomised order and perturbation points

Dynamic experiment part

1. Make sure the FSR input comes from channel 1 (FSR under heel)
2. Open an old perturbation .mat file in MrKick, and then make a new file with the settings loaded
3. Go to Settings → Event timing → Edit all, and input the perturbation timing calculated by the matlab file
4. Run the treadmill at the subject's preferred speed
5. Warn subject at the start of acquisition, and acquire 20 sweeps of perturbations (40 sweeps in all, including the non–perturbed sweeps)
6. Repeat steps 3–5 for the remaining two perturbation times

Isometric experiment part

1. Make sure the FSR input comes from channel 2 (external FSR)
2. Open an old perturbation .mat file in MrKick, and then make a new file with the settings loaded
3. Go to Settings → Event timing → Edit all, and input 0 as the perturbation timing
4. Instruct the subject to take the position of the right gait phase, using the markings and measured distances as guidance
5. Warn subject at the start of acquisition, and acquire 20 sweeps of perturbations by repeatedly pressing the external FSR
6. Repeat steps 4–5 for the remaining two perturbation times